Use Dependence of Tetrodotoxin Block of Sodium Channels: A Revival of the Trapped-Ion Mechanism

Franco Conti, Alessandra Gheri, Michael Pusch, and Oscar Moran
Istituto di Cibernetica e Biofisica, CNR, I-16149 Genoa, Italy

ABSTRACT The use-dependent block of sodium channels by tetrodotoxin (TTX) has been studied in cRNA-injected *Xenopus* oocytes expressing the α-subunit of rat brain IIA channels. The kinetics of stimulus-induced extra block are consistent with an underlying relaxation process involving only three states. Cumulative extra block induced by repetitive stimulations increases with hyperpolarization, with TTX concentration, and with extracellular Ca^{2+} concentration. We have developed a theoretical model based on the suggestion by Salgado et al. that TTX blocks the extracellular mouth of the ion pore less tightly when the latter has its external side occupied by a cation, and that channel opening favors a tighter binding by allowing the escape of the trapped ion. The model provides an excellent fit of the data, which are consistent with Ca^{2+} being more efficient than Na^+ in weakening TTX binding and with bound Ca^{2+} stabilizing the closed state of the channel, as suggested by Armstrong and Cota. Reports arguing against the trapped-ion mechanism are critically discussed.

INTRODUCTION

The guanidinium toxins tetrodotoxin (TTX) and saxitoxin (STX) are the most potent and selective blockers of sodium channels (for reviews, see Narahashi, 1974; Kao, 1986; Hille, 1992). When bound to their receptor site on the extracellular side of a channel, they prevent ions from flowing through the pathway opened by activation. Extracellular cations compete with toxin binding, Ca^{2+} and Mg^{2+} being as efficient at concentrations two orders of magnitude lower than Li^+ or Na^+ (Weigele and Barchi, 1978; Doyle et al., 1993). The permeability of sodium channels to guanidinium ions, and the fact that impermeant cations and low pH have similar antagonizing effects on sodium permeability and on toxin binding, suggested early that the toxin receptor may include the selectivity filter of the ion pore (Hille, 1975). Although a strict identification of the binding site with the selectivity filter leads to several inconsistencies (Hille, 1992), none of these argues against the general idea that the toxins block the extracellular access to the pore in a position where they may also interact with some of the structures responsible for the pore selectivity. Indeed, most modifications that produce marked changes in pore permeability also affect toxin sensitivity. In particular, single point mutations that map the toxin binding domain also have profound effects in general on pore permeability (Noda et al., 1989; Pusch et al., 1991; Terlau et al., 1991; Heinemann et al., 1992; Satin et al., 1992; Kontis and Goldin, 1993). The domain, comprising a segment of at least four amino acids in each of the four homologous repeats of the polypeptide, delineates an outer ring of polar residues that is mostly influential for toxin binding and an inner ring where mutations have stronger effects on pore permeability and selectivity. Computer-aided molecular models of this domain (Lipkind and Fozzard, 1994) show plausible barrel-like structures in which a wide extracellular vestibule of the pore may fit a TTX or a STX molecule in close-packed configurations. These hypothetical models are qualitatively similar to those suggested for the structurally related potassium channel, where the interaction of the rigidly structured charybdotoxin with its receptor has been studied by complementary mutagenesis (Stocker and Miller, 1994; Hidalgo and MacKinnon, 1995).

Although most effects of guanidinium toxins are consistent with the view that permeation of the Na^+ channel is gated by cytoplasmic structures and enabled by voltage sensors that move within the protein moiety without modifying the structure of the toxin receptor in the outer pore, some observations suggest interactions between gating and toxin binding. For example, the effect of internal organic cations on sodium gating is changed by TTX in squid axons (Cahalan and Almers, 1979; Armstrong and Croop, 1982), and sodium gating currents are sensibly modified by STX and TTX in crayfish and squid axons (Heggeness and Starkus, 1986; Keynes et al., 1991). Conversely, the efficacy with which the toxins block ion permeation is increased by stimulations that activate gating transitions (use-dependent block). In this work we examine this last phenomenon in detail.

Use dependence is a characteristic of the effects of local anesthetics and has long been taken as evidence that these drugs bind better to the open channel than to a closed one (Strichartz, 1973; Courtney, 1975; for reviews see Butterworth and Strichartz, 1990; Hille, 1992). The use dependence of guanidinium toxin block was first observed by Baer et al. (1976) in the low-toxin-sensitivity cardiac sodium channels, where it has subsequently been studied extensively (Cohen et al., 1981; Carmeliet, 1987; Eickhorn et al., 1990; Makielski et al., 1993). It appears to be a

Received for publication 13 February 1996 and in final form 15 June 1996.

Address reprint requests to Dr. Franco Conti, Istituto di Cibernetica e Biofisica, CNR, Via De Marini 6, I-16149 Genova, Italy. Tel.: 39-10-6475-592; Fax: 39-10-6475-500; E-mail: conti@barolo.icb.ge.cnr.it.

Dr. Pusch's permanent address is Zentrum für Molekulare Neurobiologie, Universität Hamburg, Germany.

0006-3495/96/09/1295/18 $2.00

common feature of STX and TTX block of all voltage-gated Na^+ channels, also being observed in highly toxin-sensitive preparations such as the crayfish axon (Salgado et al., 1986) and the frog node of Ranvier (Lönnendonker, 1989a, 1991a,b). It has also been studied in frog oocytes expressing the α-subunits of wild-type and mutated rat brain and rat heart Na^+ channels (Patton and Goldin, 1991; Satin et al., 1994a).

A distinctive feature of STX and TTX use dependence, first described by Salgado et al. (1986), is that a single brief stimulus can trigger a large extra block that develops with the characteristic kinetics of the toxin binding reaction even while the channels are kept at very negative holding potentials. This has been taken by most authors as evidence for the existence of a long-lived voltage-dependent conformation of the channel protein in which the toxin receptor has a higher binding affinity. From the observation that significant extra block can be induced by conditioning pulses that do not elicit appreciable sodium currents, Patton and Goldin (1991) suggest that such configuration occurs at an early step in the normal pathway of activation, and a kinetic scheme with a partially activated state with higher toxin binding affinity can describe the phenomenology of STX use dependence in cardiac channels (Makielski at al., 1993; Satin et al., 1994a).

Alternatively, Salgado et al. (1986) suggested that a lower resting affinity for toxin binding may arise because the toxin molecules often bind to the outer vestibule of a pore that is already hosting at a deeper site a toxin-repellent Na^+ or Ca^{2+}, which remains trapped in the pore if the cytoplasmic gate is closed. Any depolarization giving the channel a high probability of opening at least once allows the escape of the trapped ion to the intracellular medium, thereby increasing the stability of the bound state. This mechanism is supported by the notion that toxin binding is antagonized by monovalent and divalent cations (Weigele and Barchi, 1978; Doyle et al., 1993; Lönnendonker et al., 1990). An attractive feature of the "trapped-ion" model is that it does not postulate any ad hoc structural conformation of the toxin receptor. The model has been dismissed on the basis of apparent qualitative inconsistencies with the voltage dependencies of extra block (Patton and Goldin, 1991) and with the low sensitivity to separate changes of sodium (Lönnendonker, 1991b; Patton and Goldin, 1991) or calcium concentration (Satin et al., 1994a). We show in this paper that a proper quantitative account of the effects expected from the repulsion between toxins and pore-bound cations does fit our data and all known properties of the use-dependent block of sodium channels by guanidinium toxins.

Following the general idea of Armstrong and Cota (1991) that cations bound at the outer side of the selectivity filter may modify gating, we argue that other apparent toxin-gating interactions may result from the indirect effect of the toxins on the binding of cations to the closed channel.

MATERIALS AND METHODS

Oocyte preparation

Oocytes, dissected from the frog *Xenopus laevis* under anesthesia, were injected with cRNA and prepared for electrophysiological recordings following standard procedures (Methfessel et al., 1986; Stühmer et al., 1987). In brief, after removal of the follicular cell layer, eased by pretreatment with collagenase (Sigma, St. Louis, MO), the oocytes were microinjected with about 50 nl of solution containing 0.25 $\mu g/\mu l$ of cRNA encoding the α-subunit of rat brain type II Na^+ channels (Noda et al., 1986). They were then incubated in Barth's solution for 2–6 days before the measurements. For patch-clamp experiments the vitelline membrane was removed 20 min before the measurements.

Solutions

Most of the experiments described in this work were done on whole oocytes bathed in normal frog Ringer (NFR) with the following composition (in mM): 112 NaCl, 1.8 $CaCl_2$, 2.5 KCl, 10 NaOH-HEPES, pH 7.2. Extracellular solutions with different Ca^{2+} concentrations were prepared by mixing in various proportions two solutions with the following composition (in mM): 1) 115 NaCl, 10 NaOH-HEPES, 2.5 KCl, pH 7.2; 2) 107.5 NaCl, 5 $CaCl_2$, 10 NaOH-HEPES, 2.5 KCl, pH 7.2. Appropriate aliquots of a 100 μM TTX solution were added to obtain any desired TTX concentration, [T]. Patch-clamp measurements were obtained with recording pipettes filled with one of the above extracellular solutions, while the oocyte was maintained in a bathing solution that kept the cell potential within ± 2 mV and contained (in mM): KCl 110, NaCl 20, EGTA-KOH 5, Tris-Cl 10; pH 7.2. All salts were purchased from Sigma; TTX was purchased from Calbiochem (San Diego, CA) or Sigma. The oocytes were positioned in a recording chamber, with a total volume of 150 μl. Solutions were changed by perfusing 5–10 ml of precooled solutions at about 4 ml/min. Temperature was regulated by a Peltier cell in contact with the bottom of the recording chamber and measured with a thermistor (Ø 0.2 mm) placed at 1–2 mm from the oocyte. Experiments were performed at 15 ± 1°C.

Current recordings

Whole-oocyte currents were measured using a high-voltage two-electrode voltage-clamp amplifier (NPI Electronics, Tamm, Germany). The electrodes were borosilicate glass pipettes (Hilgenberg, Malsfeld, Germany) filled with a solution containing 2 M KCl, 2 mM EGTA, 10 mM HEPES, pH 7.2. They had a resistance of 0.4 to 0.8 MΩ.

Recordings from macropatches in the cell-attached configuration were obtained using an EPC-7 patch-clamp amplifier (List, Darmstadt, Germany). Patch pipettes were pulled from aluminum silicate glass capillaries (Hilgenberg), coated with silicone rubber, and heat-polished to obtain tip resistances of 0.5 to 1 MΩ when the pipettes were filled with the recording solution.

Data acquisition and analysis

Stimulation and data acquisition were controlled by a Macintosh microcomputer (Cupertino, CA) interfaced to the voltage-clamp amplifier with a 16-bit AD/DA converter (Instrutech, Elmond, NY). Currents were filtered at 5 or 10 kHz with a 4-pole low-pass Bessel filter (Ithaco, Ithaca, NY). Linear leakage and capacitive currents were subtracted off-line using the responses to pulses of 20 mV amplitude from the holding membrane potential, V_H, appropriately scaled. Positive pulses were used for V_H between -120 and -110 mV; negative ones for V_H between -100 and -60 mV. V_H was routinely kept at -120 mV, except for studies of V_H dependence. The average of 8 to 16 leakage records, obtained at the beginning and end of each stimulation sequence, were checked for any

systematic trend. The linear correction was made using the overall average of all leak records to increase the signal-to-noise ratio.

At $V_H \geq -90$ mV, high-frequency repetitive stimulations often caused some cumulative slow inactivation of the sodium currents that could bias the measurements of TTX use dependence. These effects, which were minimized by using short test pulses that caused only a partial fast inactivation, developed with time constants distinctively shorter than those of TTX use-dependent block. They were estimated from control measurements in the absence of TTX and were subtracted whenever significant.

RESULTS

Enhancement of TTX block under repetitive stimulation

The general properties of the blocking effect of TTX upon the currents carried by sodium channels and a typical paradigm of its use dependence are illustrated in Fig. 1. Fig. 1 *A* shows superimposed records of sodium currents recorded from a whole oocyte bathed in NFR before and after the addition of 20 nM TTX. All responses were elicited by the same voltage pulse of 4 ms from $V_H = -120$ mV to $V_P = -10$ mV. The traces labeled "no TTX" are 10 successive responses produced at 1-s intervals. The other traces, in order of decreasing amplitudes, are the first and every other response to a train of 50 stimulations given every second starting after a resting period of about 3 min after the addition of TTX. We interpret the relative decrease in amplitude between the responses in no TTX and the first response in 20 nM TTX (~47% in this experiment) as the TTX block probability, or tonic block, for sodium channels in resting conditions. The further gradual decrease of the responses during the train stimulation toward a new asymptotic level is called use-dependent, phasic, or extra block.

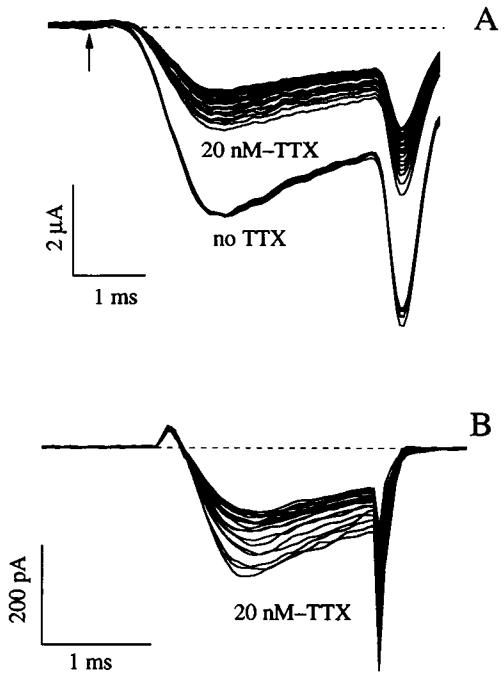

FIGURE 1 Tonic and use-dependent block of sodium currents by TTX. (*A*) Voltage-clamp records of whole-cell sodium currents recorded from the same oocyte bathed in NFR, before (no TTX) or after the addition of 20 nM TTX. All responses were elicited by the same voltage pulse of 4 ms from $V_H = -120$ mV to $V_P = -10$ mV. The application of TTX reduces the amplitude of the peak current to ~47%. Traces in 20 nM TTX show the first and every other response to a train of 50 stimulations given at 1-s intervals, starting after a quiescent period of 3 min. (*B*) Sodium currents from a cell-attached macro-patch recorded with a pipette filled by NFR with 20 nM TTX. The traces shown are the first and every other fourth response evoked by a train of 70 pulses with $V_H = -120$ mV, $V_P = +10$ mV, $T_P = 2$ ms.

Notice that the changes in amplitude caused by the addition of TTX and by the stimulation occur without any significant change in the time course of the voltage-clamp currents, during either the depolarization or the repolarization. Such mere scaling effects due to changes in the fraction of sodium channels blocked by TTX are faithfully revealed by voltage-clamp measurements in whole oocytes despite the inadequacy of this technique for recording the fast kinetics of sodium currents. This is confirmed by the fact that the stimulated enhancement of toxin block shown in Fig. 1 *A* is observed with similar characteristics when recording partially blocked sodium currents from cell-attached macropatches with much better space-clamp and time resolution (Fig. 1 *B*). Macropatch recordings were used only occasionally in our present study because they are much noisier and do not allow control measurements before the addition of TTX to test the resting potency of the toxin. They were essential, however, for testing the effects of very large depolarizations, described later in Fig. 7.

Increasing the frequency of stimulation increases the amount of block enhancement and hastens its development. Fig. 2 shows the results of an experiment similar to that of Fig. 1 *A* on a different oocyte exposed to several train stimulations differing only for the pulse interval, ϑ. The fraction of unblocked channels relative to resting conditions, estimated by the ratio of peak currents, $I(t)/\bar{I}$, is plotted in Fig. 2 *A* as a function of the time of stimulation, t. The peak current before the addition of TTX, indicated in the following by $\bar{I}_0$, did not decay appreciably for train stimulations with pulse intervals of 1 s (filled symbols), demonstrating the absence of intrinsic cumulative-inactivation processes. The data in 20 nM TTX were least-squares fitted with single exponentials, drawn as continuous lines, according to

$$\frac{I(t)}{\bar{I}} = 1 - B_\vartheta(1 - e^{-t/\tau_\vartheta}), \qquad (1)$$

where $B_\vartheta = (\bar{I} - I_\infty)/\bar{I}$, with I_∞ indicating the asymptotic value of the peak current, is the asymptotic percentage decrease in the number of unblocked channels, usually described as an extra block probability. The ϑ dependencies of the fitted parameters B_ϑ and τ_ϑ, obtained from the experiment in Fig. 2 *A*, are shown in Fig. 2, *B* and *C*. As the pulse interval was decreased, B_ϑ increased toward an upper limit of ~0.45, whereas τ_ϑ decreased toward a lower limit of ~18 s. These limiting values, describing the properties of

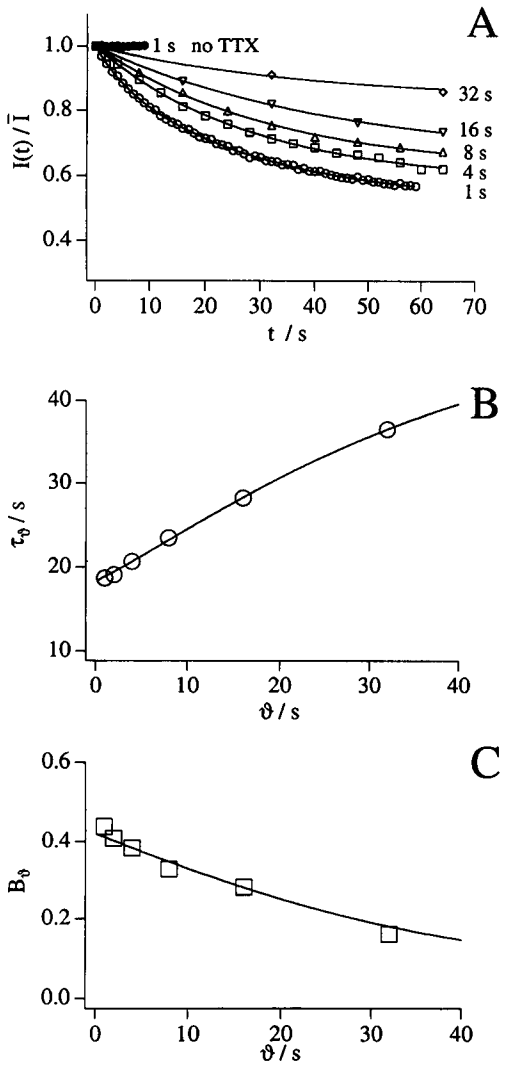

FIGURE 2 Dependence of cumulative extra-block on stimulation frequency. (*A*) Plot of the decay of the peak amplitude normalized to the first response, $I(t)/\bar{I}$. ● (labeled "no TTX"), 10 successive responses produced at 1-s intervals in NFR. Other symbols refer to responses recorded in the same oocyte after the addition of 20 nM TTX, for train stimulations (V_H = −120 mV, V_P = 0 mV, T_P = 3.5 ms) with different impulse intervals, ϑ, indicated in the figure. Smooth lines are the least-squares fits of the data according to Eq. 1 with B_ϑ = 0.44, τ_ϑ = 18.7 s (ϑ = 1 s); B_ϑ = 0.38, τ_ϑ = 20.7 s (ϑ = 4 s); B_ϑ = 0.33, τ_ϑ = 23.5 s (ϑ = 8 s); B_ϑ = 0.28, τ_ϑ = 28.2 s (ϑ = 16 s); B_ϑ = 0.16, τ_ϑ = 36.6 s (ϑ = 32 s). (*B*) Time constant of the extra block. τ_ϑ is given as a function of the interpulse interval ϑ. The limiting time constant for $\vartheta \to 0$ is τ = 18.2 s. (*C*) Plot of the asymptotic extra-block, B_ϑ, as a function of the interpulse interval ϑ. The limiting value for $\vartheta \to 0$ is B_e = 0.43. The continuous lines represent the fit of the data with Eqs. A7–A9 yielding estimates for the rate constants, λ_1 and λ_2, of 0.016 s^{-1} and 0.14 s^{-1}, respectively.

saturated extra block, are indicated in the following with B_e and τ. They varied substantially with TTX concentration and other parameters, but in all conditions of our study (and for $V_P \geq -10$ mV) they were practically reached for stimulation frequencies ≥ 1 Hz.

The lower limit of τ_ϑ means that the increase of TTX block observable 1 s after a pulse to $V_P \geq -10$ mV is hardly enhanced by other pulses given in between. This implies that the effect of each pulse is intrinsically rate limited and must proceed to a significant extent for repriming to be effective. These features are predicted by the trapped-ion model described by Scheme 1:

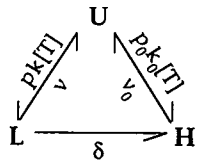

Scheme 1

where U represents the toxin-free channel, which may host a cation in its outer pore lumen, with very fast kinetics and with probability p; L represents a blocked state of the channel in which a TTX molecule is bound to the outer vestibule of the pore on top of a trapped cation; H is an alternative blocked state that more tightly binds a toxin molecule that has met its receptor site while (with probability $p_0 = 1 - p$) the pore was cation-free. The rate constants for TTX association and dissociation are assumed to be independent of voltage, and, consistently with the definition of states L and H, it is expected that $k \leq k_0$ and $\nu > \nu_0$. Experiments on crayfish axons (Salgado et al., 1986) and on rat brain channels expressed in oocytes (Satin et al., 1994b) indicate that toxin binding, as revealed by tonic block measurements for $V_H < -100$ mV, may be intrinsically voltage dependent. However, such dependence (a doubling of toxin affinity for about 100 mV hyperpolarization) is very mild in comparison with the effects considered in this work (see Fig. 4), which are attributed in our model to the modulation by voltage of the rate, δ, of L→H transitions. We assume $\delta = 0$ at large resting hyperpolarizations that keep the channels tightly closed. However, because the mean open time at $V_H \geq -100$ mV is longer than 50 μs (Hirschberg et al., 1995), almost any opening of a channel in state L is likely to cause the escape of the trapped cation, switching the channel to state H (even in the absence of a repelling TTX molecule, Na^+ can travel across the pore in less than 0.2 μs, and Ca^{2+} is unlikely to be more than 100 times slower).

In the above model, the immediate consequence of a depolarizing pulse is the loss of trapped cations by channels in state L, which creates an imbalance between the rate of TTX association (which is not changed) and that of TTX dissociation (which is now lower because it occurs only from cation-free channels). Therefore, the increase in the number of blocked channels is intrinsically rate-limited by the toxin-binding reaction, and repriming can be effective only after a new significant build-up of blocked channels in state L.

The expressions of the parameters B_e and τ predicted by Scheme 1 can be derived as follows. According to Scheme 1, the resting fraction of unblocked currents, $\bar{I}/\bar{I}_0$, i.e., the

steady-state probability of the unblocked state U, is given by (see Appendix):

$$\frac{\bar{I}}{\bar{I}_0} = \frac{1}{1 + A_t[T]}, \tag{2}$$

where the tonic block affinity, A_t, is defined by

$$A_t = p_0 \frac{k_0}{\nu_0} + p \frac{k}{\nu + \delta} \frac{\nu_0 + \delta}{\nu_0}. \tag{3}$$

Saturated extra block develops during train stimulations that repetitively deplete the pool of channels in state L at a much higher rate than U→L transitions. Then TTX can bind to the channels with its highest affinity without effectively suffering the repulsion from trapped cations. These conditions correspond to the limit $\delta \to \infty$, where scheme 1 becomes

$$\mathrm{U} \underset{\nu_0}{\overset{(pk + p_0k_0)[T]}{\rightleftharpoons}} \mathrm{H}$$

Scheme 2

It is easily verified that the steady-state (asymptotic) fraction of unblocked currents, $I_\infty/\bar{I}_0$, is expected in this case to be given by

$$\frac{I_\infty}{\bar{I}_0} = \frac{1}{1 + A_M[T]}, \tag{4}$$

where A_M is the saturated (maximum) affinity for TTX binding defined by

$$A_M = \frac{p_0k_0 + pk}{\nu_0}. \tag{5}$$

Furthermore, the relaxation of the unblocked currents from $\bar{I}$ to I_∞, following the onset of the new conditions of Scheme 2, is a single exponential with time constant τ, given by

$$\tau = \frac{1/\nu_0}{1 + A_M[T]}. \tag{6}$$

Finally, using Eqs. 2 and 4, the extra block parameter, $B_e = (\bar{I} - I_\infty)/\bar{I}$, is expressed by

$$B_e = B_i \frac{A_M[T]}{1 + A_M[T]}, \tag{7}$$

where

$$B_i = \frac{A_M - A_t}{A_M} \tag{8}$$

is the fraction of saturable binding affinity inhibited at resting conditions. The consistency of the predictions of Scheme 1 for the [T] dependencies of tonic and use-dependent block with the experimental observations is discussed later.

Equation 7 shows explicitly that according to Scheme 1 the extra block parameter B_e in fact measures the extent of a tonic block inhibition. Using Eqs. 3 and 5, the inhibited block can be expressed as

$$B_i = p \frac{\nu}{\nu + \delta} \frac{k}{p_0k_0 + pk} B_i^*, \tag{9}$$

where

$$B_i^* = 1 - \frac{\nu_0}{\nu} \tag{10}$$

characterizes the maximum inhibition, approached for full cation occupancy ($p = 1$) and at large negative V_H ($\delta \to 0$).

Kinetics of stimulated block enhancement

The actual time course of the transient block increase triggered by a single stimulus is measured in double-pulse experiments such as that shown in Fig. 3 *A*. The data, from an oocyte bathed in NFR with 50 nM TTX and kept at $V_H = -120$ mV, show the ratio of the responses elicited by two identical pulses ($V_p = -10$ mV; $T_p = 5$ ms) as a function of the time interval, t, between the pulses. A resting period of ~3 min was allowed before each double pulse protocol. The smooth line in Fig. 3 *A* is the least-squares fit of the data according to

$$\frac{I(t)}{\bar{I}} = 1 - C(e^{-\lambda_1 t} - e^{-\lambda_2 t}). \tag{11}$$

and was obtained for $C = 0.26$, $\lambda_1 = 0.020\ s^{-1}$, and $\lambda_2 = 0.23\ s^{-1}$. The relatively large size and the biphasic time course of the extra block induced by a single pulse are the most prominent features of the use-dependent block by guanidinium toxins. The data of Fig. 3 *A* are similar to those first observed by Salgado et al. (1986) for STX block in crayfish axons, and confirmed by others for STX and TTX in other nerve and cardiac preparations (Lönnendonker, 1989a; Patton and Goldin, 1991; Makielski et al., 1993). In particular, our rate constants at 15°C are about three times lower than those obtained by Patton and Goldin (1991) on the same preparation, at 20–22°C and for comparable TTX concentrations.

The fact that two rate constants are sufficient to fit the data of Fig. 3 *A* is consistent with an underlying process like that described by Scheme 1, which involves only transitions between three states. The time-dependent general solution of Scheme 1, the relationship between the rates λ_1 and λ_2, and the parameters of the scheme are given in the Appendix. Qualitatively, a brief pulse given after long resting conditions upsets almost instantaneously the steady distribution of channels between the three states, allowing the fast L→H conversion of a significant fraction of channels. The ensuing relaxation process is initially dominated by the new recruitment of blocked channels via U→L transitions and subsides later, mainly via the slower backward transitions from H to

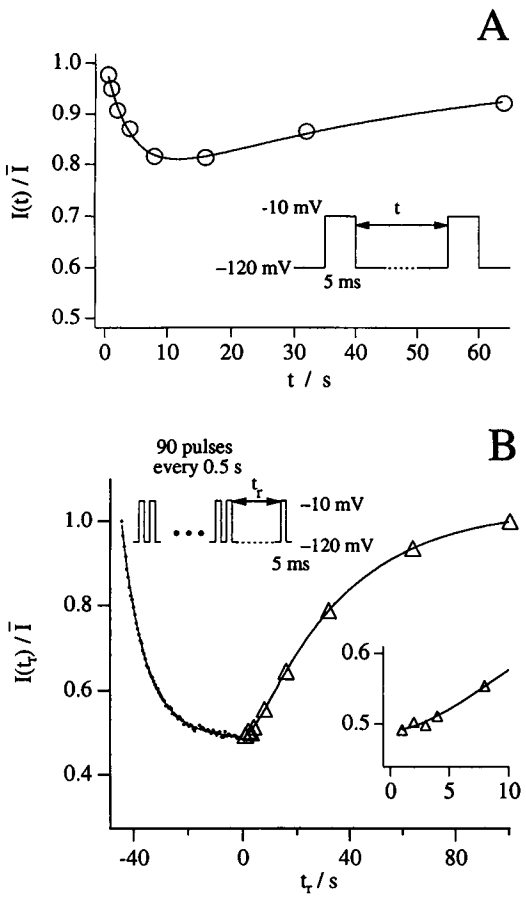

FIGURE 3 The onset and recovery of extra block is a double-exponential relaxation process. Data in *A* and *B* are from the same oocyte bathed in NFR with 50 nM TTX and kept at $V_H = -120$ mV between stimulations. Conditioning and test pulses were at $V_P = -10$ mV; $T_P = 5$ ms. (*A*) The ratio of the responses elicited by two successive pulses, $I(t)/\bar{I}$, starting from resting conditions, is plotted versus the time of interpulse, t. The data are least-squares fitted by the smooth line according to Eq. 11, with $C = 0.26$, $\lambda_1 = 0.020\ s^{-1}$, and $\lambda_2 = 0.23\ s^{-1}$. (*B*) Recovery from the extra block built up by a repetitive stimulation with a train of 90 pulses at 0.5-s intervals. The exponential decay of the response amplitude during the conditioning train (shown as *dots*) is fitted by Eq. 1, with $B_e = 0.49$ and $\tau = 9.1$ s. After the last pulse of the train a recovery time, t_r, was allowed before applying another (test) pulse, eliciting a response whose amplitude relative to resting conditions is shown as triangles. The *inset* shows that the initial part of the recovery has a delay due to the biphasic nature of the phenomenon. The continuous line is the least-squares fit of these data with Eq. 12, obtained for $B_e = 0.50$, $\lambda_1 = 0.029\ s^{-1}$, and $\lambda_2 = 0.24\ s^{-1}$.

U. The actual amplitude of the biphasic relaxation is obtained from the additional condition that the pulse causes a conditional probability π that a channel in state L opens at least once, losing the trapped ion and switching to state H. Under this condition, the predicted amplitude coefficient in Eq. 11 is (see Appendix)

$$C = \pi B_i A_M[T] \frac{\nu_0}{(\lambda_2 - \lambda_1)}. \quad (12)$$

Thus, as expected intuitively, the transient block enhancement is proportional both to the amount of tonic inhibition B_i and to the probability π that such inhibition is momentarily removed by the pulse.

Furthermore, the retrieval of unblocked channels after having imposed saturating block conditions is consistent with a simple three-state process. Fig. 3 *B* shows the results of this type of measurement performed on the same oocyte of Fig. 3 *A*, with [T] = 50 nM. The protocol consisted of a train of 90 pulses with $\vartheta = 0.5$ s, followed by a single test pulse applied after a recovery time t_r from the last pulse of the train. It was repeated with different t_r values between 1 and 100 s, allowing 3 min for the reestablishment of resting conditions each time. The figure shows the peak currents recorded during one of the trains (*dots*) and the test response for each t_r (*triangles*), normalized to the first response of the respective train to correct for rundown (~ 20% in 30 min in this experiment). The continuous line through the dots is the single exponential fit of the cumulative extra block already described, yielding $B_e = 0.49$ and $\tau = 9.1$ s. The line through the triangles is the least-squares fit with

$$\frac{I(t_r)}{\bar{I}} = 1 - B_e \frac{\lambda_2 e^{-\lambda_1 t_r} - \lambda_1 e^{-\lambda_2 t_r}}{\lambda_2 - \lambda_1} \quad (13)$$

obtained for $\lambda_1 = 0.029\ s^{-1}$ and $\lambda_2 = 0.23\ s^{-1}$. The data of Fig. 3 *B* are very similar to those reported by Makielski et al. (1993) for the phasic block of cardiac sodium channels by STX, except that the kinetics of the latter process are about 10 times faster and the recovery was fitted by these authors with a single exponential. The *inset* of Fig. 3 *B* shows that the effect of the fast component is a short delay in the recovery. This may be difficult to reveal in a preparation where the rate of the fast component is close to that of recovery from inactivation.

The analysis of the time-dependent solution of scheme 1 also allows predictions for the parameters B_ϑ and τ_ϑ that characterize the use-dependent block caused by train stimulations with pulse intervals, ϑ, that are comparable to or longer than the characteristic times of the toxin-binding reactions. During such pulse protocols, the percentage of unblocked channels in each interval follows a double-exponential relaxation, but the initial conditions are determined by the previous history of the system. As shown in the Appendix, in this case we can write and solve a recurrent relation linking the U-state probabilities at the times of application of two successive pulses. The predicted decrease in unblocked currents is indeed a single exponential, as in Eq. 1. The expressions of the asymptotic relative decrease, B_ϑ, and of the time constant, τ_ϑ, as a function of the stimulation interval ϑ, are given in the Appendix by Eqs. A7–A9. They contain as parameters the two limiting values B_e and τ and the characteristic rates, λ_1 and λ_2, and we have used these expressions to get independent estimates of these rates from data of the type shown in Fig. 2. The solid lines in Fig. 2 are least-squares fits of the data with these theoretical expressions, yielding for that situation $\lambda_1 = 0.016\ s^{-1}$ and $\lambda_2 = 0.14\ s^{-1}$.

Table 1 summarizes our fitted estimates of the kinetic parameters of use dependence, obtained from the above three different protocols. It is seen that for the same [T] the different methods yield comparable estimates of λ_1 and λ_2, which increase with [T], consistently with two of the rate constants of Scheme 1 being directly proportional to [T]. A less intuitive prediction of Scheme 1 (see Appendix) is that the sum of the characteristic rates and the rate of saturated extra block increase with [T] by the same amount, so that the quantity $(\lambda_1 + \lambda_2 - 1/\tau)$ is independent of [T]. The last column of Table 1 shows that the data are in good agreement with that prediction.

Voltage dependence

The amount of stimulated block enhancement decreases at less negative holding potentials. This is illustrated in Fig. 4 *A* (*open squares*) for an experiment in NFR with 30 nM TTX (see also Fig. 6 *B* for the dependence of the effect on calcium concentration). It is seen that the asymptotic extra block of ~50%, measured at $V_H = -120$ mV, is reduced to 5% for $V_H = -60$ mV. Also shown is the opposite effect on tonic block: the resting fraction of peak currents abolished by the toxin increases with V_H. The latter data are subject to a relatively large error, because they involve the comparison of measurements with and without toxin taken tens of minutes apart. Nevertheless, it is obvious that both tonic and extra block change drastically in the same V_H range (from -80 to -60 mV) and that the increase in tonic block caused by steady depolarizations to $V_H = -60$ mV is comparable to the stimulated extra block at $V_H \leq -100$ mV. These results agree with previous reports on frog nodes, where TTX and STX use dependencies become readily noticeable

TABLE 1 Kinetic parameters of TTX use-dependent block evaluated from three different protocols at $V_H = -120$ mV and at different [T]

Protocol	[T] (nM)	λ_1 (s^{-1})	λ_2 (s^{-1})	τ (s)	$\lambda_1 + \lambda_2 - 1/\tau$
TR	20	0.015	0.19	18.2	0.15
TR		0.016	0.14	18.3	0.10
TR		0.014	0.20	21.0	0.17
DP		0.015	0.19	—	
DP		0.014	0.19	—	
DP		0.017	0.15	—	
RE		0.027	0.19	—	
Mean ± SD		0.017 ± 0.005	0.18 ± 0.02	19.2 ± 1.6	0.14 ± 0.03
TR	50	0.022	0.23	8.9	0.14
TR		0.035	0.28	7.0	0.17
DP		0.020	0.23	—	
DP		0.047	0.27	—	
RE		0.029	0.24	—	
RE		0.057	0.27	—	
Mean ± SD		0.035 ± 0.015	0.25 ± 0.02	7.95	0.155

TR, Data from fits of the dependence of B_ϑ and τ_ϑ on the stimulation intervals ϑ; DP, data from double pulse protocols; RE, data of recovery from saturated extra block.

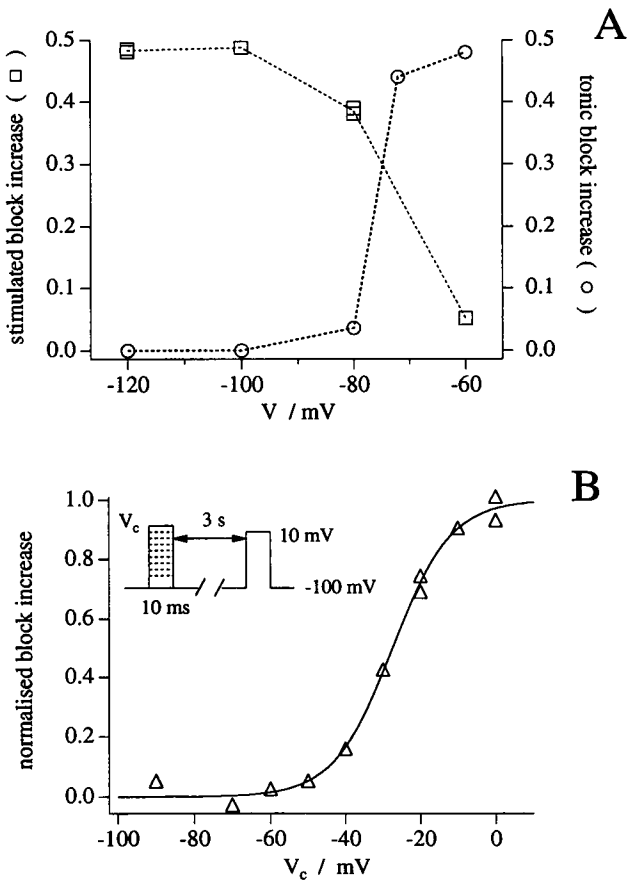

FIGURE 4 Dependence of TTX block on membrane potential. (*A*) Asymptotic cumulative extra-block (□) and the increase in tonic block (○) as a function of the holding potential, V_H. The cumulative extra-block was induced by trains of 8 ms pulses to $V_P = -10$ mV at 1-s intervals; changes in tonic block were estimated by comparing peak currents evoked by a single pulse before and after addition of the toxin ([T] = 30 nM). Notice that both the reduction of cumulative extra-block and the increase in tonic block with V_H occur between -80 and -60 mV. A Boltzmann fit to the pooled data of cumulative extra-block obtained from 12 oocytes in NFR and [T] = 20 nM yielded a mid-voltage of -64 mV and a slope factor of 11 mV. (*B*) Normalized extra-block induced by a single conditioning pulse of variable amplitude, V_c. The conditioning pulse was followed by a test pulse ($V_P = 10$ mV) after an interpulse of 3 s. The solid line is a fit of the data with a Boltzmann function, with a mid-voltage of -28 mV and a slope factor of 7 mV.

only for $V_H < -70$ mV (Lönnendonker, 1989a) and where the saturating block under repetitive stimulation is voltage independent (Lönnendonker, 1989b). Likewise, for the same preparation used in this work, Patton and Goldin (1991) report that maximum TTX block is achieved indifferently under saturating stimulations at $V_H = -100$ mV or at a steady polarization of -60 mV.

The data of Fig. 4 *A* are consistent with the idea of Scheme 1 that use-dependent block arises from the removal of a tonic inhibition of toxin binding and that moderate steady depolarizations per se can antagonize such inhibition. According to Eq. 9, tonic block inhibition, and thus saturated extra block, are halved at holding potentials that allow a steady rate of channel openings, δ, equal to the rate

ν of TTX dissociation from a cation-occupied channel, and vanish for $\delta \gg \nu$. Increasing δ causes the transition from a regime in which most bound toxins dissociate from their receptors before the respective channel has had any chance of opening, to one in which any blocked channel opens at least once before losing the blocking particle. In substantial agreement with the data of Fig. 4 *A*, we expect this transition to occur in the interval -90 mV $\leq V_H \leq -50$ mV, where we estimate from the single-channel data of Hirschberg et al. (1995) that δ increases from 10^{-2} s^{-1} to 0.7 s^{-1}, crossing the range of our estimates of the rates of TTX dissociation (between 0.04 and 0.1 s^{-1}; see Table 2).

In contrast with the steep dependence of tonic block and saturated extra block in a range of holding potentials where sodium channels tend to inactivate, the dependence on pulse amplitude of the transient extra block induced by short stimulations follows a dose-response curve similar to that of activation of sodium currents. In five experiments of the type shown in Fig. 4 *B*, the voltage inducing 50% of the maximum extra block with 10-ms pulses was -28 ± 3 mV, and the effect increased with a Boltzmann slope factor of 7 ± 1 mV. Equivalent parameters for the activation of peak sodium conductance are -16 ± 7 mV and 10 ± 1 mV (Stühmer et al., 1989). Thus, the induction of extra block occurs at slightly more negative voltages and has a slightly steeper voltage dependence than the activation of sodium conductance. These data agree with those reported by Patton and Goldin (1991), who find in addition that a mutation shifting the activation of channel conductance has a similar effect on extra block, whereas another mutation that strongly modifies inactivation is ineffectual on TTX use dependence. The lack of correlation between pulse-induced extra block and inactivation is also demonstrated by the fact that short pulses that do not cause any marked inactivation can induce maximum extra block at sufficiently high voltages (Salgado et al., 1986; Eickhorn et al., 1990; Patton and Goldin, 1991; our own data, not shown).

As discussed previously, the amplitude of the transient extra block predicted by Scheme 1 is proportional to the probability π that a channel in state L opens at least once during the pulse (Eq. 12). An accurate estimate of the dependence of π on the voltage and duration of the pulse requires data of latencies to first openings (as, e.g., in Horn et al., 1984) that are not directly available for our channels. However, taking the time to peak of the macroscopic currents as a fair estimate of the mean latency to a first opening, we expect that pulses longer than that time may yield a large π even for small peak open-channel probabilities. By a similar argument, we notice that the data of Hirschberg et al. (1995) for our channels show, at -50 mV and in the absence of inactivation, a mean open time of $\sim$220 μs and an open probability of $\sim 3.5 \times 10^{-2}$, i.e., an opening rate of 160 s^{-1}. Apart from a short delay due to transitions between closed states, we expect that a 4-ms pulse to -50 mV yields $\pi \approx 0.5$, although activating at most 3.5% of the maximum macroscopic conductance. Thus, a threshold for induction of extra block lower than that of activation of sodium conductance is fully consistent with our model.

Dependence on TTX concentration

The block of the sodium currents under stationary conditions increases with TTX concentration, [T], as expected if a single TTX molecule can block one sodium channel by binding to a single site (Hille, 1992; Ulbricht et al., 1986). Fig. 5 *A* shows the results of one experiment in which the same oocyte was tested for sodium current availability at $V_H = -120$ mV successively for [T] = 0, 5, 10, 20, and 50 nM and again at [T] = 0. The whole series of measurements took about 30 min, the final currents at [T] = 0 were about 20% smaller than the initial ones, and the measurements were corrected assuming a linear rundown. The tonic percentage of toxin-free channels was estimated from the peak current, $\bar{I}$, elicited by the same test pulse ($V_P = -10$ mV; $T_P = 7$ ms) after at least 3 min of rest from any preceding stimulation or complete exchange of solution. The smooth line in Fig. 5 *A* was drawn according to Eq. 2 for a tonic affinity, $A_t = 46\ \mu M^{-1}$, corresponding to a TTX half blocking concentration (IC_{50}) of 22 nM. In NFR and for -120 mV $\leq V_H \leq -100$ mV, A_t estimates from the tonic block at single [T] values in 15 oocytes ranged between 35 and 70 μM^{-1} with a mean value of 49 μM^{-1}, corresponding to $IC_{50} \approx 20$ nM. This is in fair agreement with previous studies of rat brain sodium channel II expressed in oocytes (Noda et al., 1989; Terlau et al., 1991).

Fig. 5 *B* shows the saturated extra block observed in the same experiment at various [T] values. It is clearly seen that increasing [T] increases the amount of stimulated block enhancement and hastens its development. Monoexponential fits according to Eq. 1 yielded B_e values increasing from 0.27 to 0.55, and τ values decreasing from 39 s to 9 s, for [T] increasing from 5 to 50 nM. These dependencies are shown in Fig. 5, *C* and *D*, where the smooth lines through the data are drawn according to Eqs. 7 and 6, respectively, for $A_M = 121\ \mu M^{-1}$, $B_i = 0.62$, and $\nu_0 = 0.016$ s^{-1}. Notice that the first two of the above parameters, and the A_t value that fits the tonic block data of Fig. 5 *A* from the same experiment, exactly fulfill Eq. 8. Indeed, the smooth lines fitting the data of Fig. 5, *A–C*, were obtained from the best

TABLE 2 Estimates of the parameters of Scheme 3

(1) ν_0 (10^{-3} s^{-1})	(2) $k_0 = k_{Na} = k_{Ca}$ (μM^{-1} s^{-1})	(3) ν_{Ca}/ν_0	(4) ν_{Na}/ν_0	(5) K_{Ca} (mM)	(6) K_{Na} (mM)
19 ± 6	2.08 ± 0.37	4.4 ± 0.9	1.8 ± 0.2	0.16 ± 0.08	34 ± 5*

*Data from Na^+ competition with STX binding (Weigele and Barchi, 1978).

fit of the combined three sets of data imposing the latter relationship. Equations 6 and 7 were fitted to 63 pooled extra block data, obtained in NFR for $V_H \leq -100$ mV and for [T] values from 5 to 100 nM. The parameters yielding the least-squares fit and their estimated errors were $A_M = 112 \pm 15\ \mu M^{-1}$; $B_i = 0.66 \pm 0.07$, $\nu_0 = 0.019 \pm 0.006\ s^{-1}$.

Dependence on extracellular Ca^{2+} concentration

The first obvious effect on TTX block of changing the extracellular Ca^{2+} concentration, [Ca], is that tonic block inhibition, as measured by the maximum extent of inducible use-dependent block, increases with [Ca]. This is shown in Fig. 6 *A* for measurements of saturated extra block at $V_H = -120$ mV and [T] = 20 nM, performed on the same oocyte bathed in three different solutions with [Ca] = 0.9, 1.8, or 5 mM. The continuous lines through the data are least-squares fits with single exponentials obtained for B_e values increasing with [Ca] from 0.35 to 0.54 and for time constants that ranged between 16.5 and 17.5 s with no systematic trend. Before discussing further these results we first digress on the effects of [Ca] on the voltage dependence of TTX block.

In the same experiment of Fig. 6 *A*, very similar measurements were obtained at $V_H = -100$ mV, showing that the V_H dependence illustrated in Fig. 4 *A* saturated for $V_H \leq -100$ mV. However, the depolarized range of V_H where B_e started to decline varied considerably with [Ca]. Fig. 6 *B* shows plots of the V_H dependence of the extra block parameter, B_e, normalized to the value measured at $V_H = -120$ or -110 mV. The data were obtained in 20 nM TTX from four oocytes at [Ca] = 0.1 mM, and from five oocytes at [Ca] = 5 mM. It is seen that increasing [Ca] from 0.1 to 5 mM shifts the V_H of half-maximum cumulative extra block by about +26 mV. As in Fig. 4 *A*, an increase in tonic block with V_H, correlated with a decrease of B_e, was observed at all calcium concentrations. In one experiment at [Ca] = 0.1 mM, comparing the steady sodium current availability with or without 30 nM TTX in the bath showed that more than 50% of the increase in tonic block occurred between -90 and -80 mV, whereas in two similar experiments at [Ca] = 5 mM the steepest change occurred between -60 and -50 mV. In one experiment of the type in Fig. 4 *B* at [Ca] = 5 mM we found, in addition, that the voltage dependence of the extra block induced by brief stimuli was shifted positively (by 10 mV) relative to that at [Ca] = 1.8 mM. Thus, increasing [Ca] causes a general shift of all voltage dependencies of extra block comparable to that observed for the activation of sodium conductance in oocytes expressing rat brain IIA channels (Pusch, 1990), which is consistent with the idea that the inducement of extra block is simply correlated with channel opening.

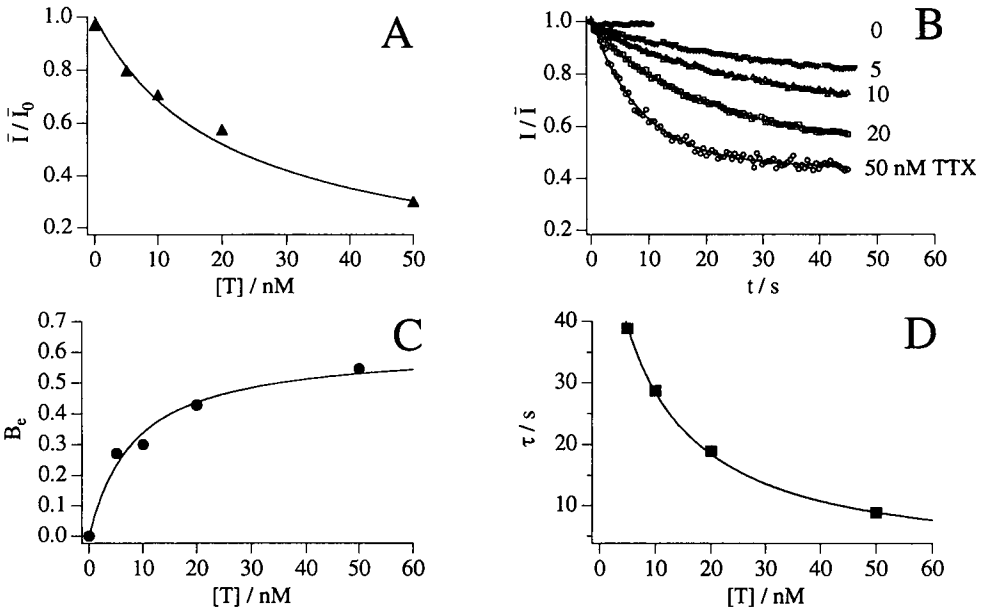

FIGURE 5 Dependence of tonic- and extra-block on TTX concentration, [T]. All data were obtained from the same oocyte bathed in NFR and exposed successively to four increasing [T] values. The oocyte was kept in resting conditions for at least 3 min after any complete exchange of solution, and 82% of the initial currents were recovered after final wash at [T] = 0. All responses were elicited by the same voltage pulse of 7 ms from $V_H = -120$ mV to $V_P = -10$ mV. (*A*) Plot of the peak response under resting conditions, normalized by the peak current measured without TTX, $\bar{I}/\bar{I}_0$. The smooth line is drawn according to Eq. 2, with $A_t = 46\ \mu M^{-1}$, corresponding to $IC_{50} \approx 22$ nM. (*B*) Time course of the peak amplitude measured during a train stimulation at 2 Hz, normalized to the first pulse, $I(t)/\bar{I}$. ●, Peak currents recorded before perfusion with TTX-containing solutions. Smooth lines are single-exponential fits according to Eq. 1. The asymptotic value and the time constant of the cumulative extra-block, B_e and τ, are plotted in *C* and *D* as a function of [T]. The smooth curves in *A*, *B*, and *C* are simultaneous least-squares fits of the data according to Eqs. 2, 6, and 7, obtained for $A_t = 46\ \mu M^{-1}$, $A_M = 121\ \mu M^{-1}$, $\nu_0 = 0.016\ s^{-1}$, and $B_i = 0.62$.

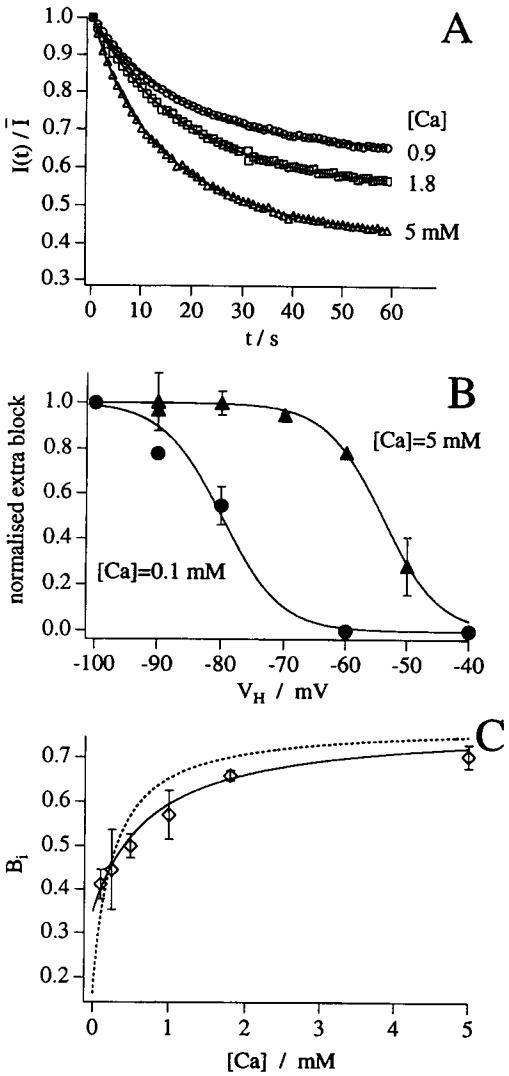

FIGURE 6 Effect of extracellular Ca^{2+} concentration, [Ca], on TTX use-dependence. (*A*) Cumulative extra-block measured on the same oocyte at [T] = 20 nM in solutions with [Ca] = 0.9, 1.8, and 5 mM. Data were taken at $V_H = -120$ mV. Smooth lines are least-squares fits according to Eq. 1, with $B_e = 0.35$, $\tau = 17.3$ s ([Ca] = 0.9 mM); $B_e = 0.44$, $\tau = 17.5$ s ([Ca] = 1.8 mM); $B_e = 0.54$, $\tau = 16.5$ s ([Ca] = 5 mM). (*B*) Dependence of cumulative extra-block on holding potential, V_H, at high and low [Ca]. The data are normalized to the values measured at $V_H \leq -100$ mV. The solid lines fit arbitrarily the data with Boltzmann functions, yielding the same slope factor of 4.6 mV and a mid-voltage of −80 mV for [Ca] = 0.1 mM and −54 mV for [Ca] = 5 mM. (*C*) [Ca] dependence of the tonic inhibition of TTX binding, B_i, estimated from cumulative extra-block at $V_H \leq -100$ mV. The number of data used to estimate B_i were 14, 3, 11, 6, 63, and 12, respectively, for [Ca] = 0.1, 0.25, 0.5, 0.9, 1.8, and 5.0 mM. B_i data, weighted according to their standard deviation (shown by bars), were best fitted with Eq. 22 (continuous line) with [Na] = 120 mM, $K_{Na} = 34$ mM, $B_i^{Na} = 0.45 \pm 0.06$ μM^{-1}, $B_i^{Ca} = 0.78 \pm 0.04$ μM^{-1}, and $K_{Ca} = 0.16 \pm 0.08$ mM. The broken line shows the expected [Ca] dependence of B_i according to the above parameters for [Na] = 20 mM.

Coming back to the data of Fig. 6 *A*, we notice first that the time constant of extra block development seems to be independent of [Ca]. At all TTX concentrations, measurements of τ at [Ca] values ranging from 0.1 to 5 mM did not show any systematic trend. According to Eq. 6, this implies in our model that the saturated binding affinity, A_M, is insensitive to [Ca]. Consistently, the [T] dependence of B_e at various [Ca] values was also reasonably well fitted by Eq. 7 using the same estimate of A_M obtained from the data in NFR solutions reported above. According to Eq. 5 (see also Eq. 16 below) the invariance of A_M is expected if the "on" rate of TTX binding is not influenced by cations occupying the outer pore lumen, i.e., if TTX is not significantly repelled by a bound cation before it has crossed the free-energy barrier for "on" binding.

The [Ca] dependence of the tonic block inhibition, B_i, estimated from measurements of saturated extra block at $V_H \leq -100$ mV, assuming a fixed $A_M = 112$ μM^{-1}, is shown in Fig. 6 *C*. Notice that the inhibited block increases monotonically with [Ca], but clearly does not vanish for vanishingly small [Ca] values. We interpret this result as implying that, besides Ca^{2+}, extracellular Na^+ can also antagonize TTX binding, although to a lesser extent. Therefore, a minimum scheme of TTX binding at low [Ca] must include the competitive binding of Na^+ and Ca^{2+} to the same site in the outer pore, with dissociation constants K_{Na} and K_{Ca}, and two distinct low-affinity blocked states:

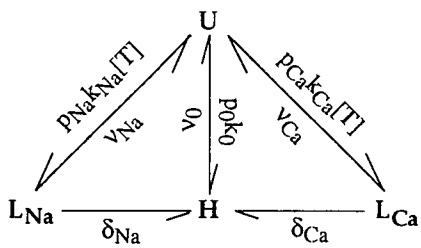

Scheme 3

where the conditional probabilities of cation occupancy of a toxin-free channel are given by

$$p_0 = \frac{1}{1 + ([Na]/K_{Na}) + ([Ca]/K_{Ca})}; \quad p_{Na} = \frac{[Na]}{K_{Na}} p_0;$$

$$p_{Ca} = \frac{[Ca]}{K_{Ca}} p_0. \quad (14)$$

It is easily verified that the steady-state probability of the unblocked state U in Scheme 3 is still given by Eq. 2, with A_t (at large negative V_H, such that $\delta_{Na} = \delta_{Ca} = 0$) given by

$$A_t = p_0 \frac{k_0}{\nu_0} + p_{Na} \frac{k_{Na}}{\nu_{Na}} + p_{Ca} \frac{k_{Ca}}{\nu_{Ca}}. \quad (15)$$

For saturating train stimulations, we can reason as before that Scheme 3 reduces to a two-state scheme like Scheme 2, except that the U→H transition rate is given in this case by $p_0 k_0 + p_{Na} k_{Na} + p_{Ca} k_{Ca}$. Therefore, we expect saturated extra block to develop as a single exponential with the asymptotic fraction of the unblocked current and the time

constant, τ, still expressed by Eqs. 4 and 6, except that A_M is given in this case by

$$A_M = \frac{p_0 k_0 + p_{Na} k_{Na} + p_{Ca} k_{Ca}}{\nu_0}. \quad (16)$$

Consequently, Eq. 7 also applies to Scheme 3, which predicts, according to Eqs. 8, 15, and 16, a tonic block inhibition given by

$$B_i = \frac{p_{Na} k_{Na} B_i^{Na} + p_{Ca} k_{Ca} B_i^{Ca}}{p_0 k_0 + p_{Na} k_{Na} + p_{Ca} k_{Ca}}, \quad (17)$$

where the maximum specific inhibitions, B_i^{Na} and B_i^{Ca}, are

$$B_i^{Na} = 1 - \frac{\nu_0}{\nu_{Na}},$$

and

$$B_i^{Ca} = 1 - \frac{\nu_0}{\nu_{Ca}}. \quad (18)$$

A simplified form of Eq. 17 is obtained if we assume that the "on" binding rates of TTX are insensitive to pore occupancy by cations, i.e.,

$$k_0 = k_{Na} = k_{Ca}. \quad (19)$$

Then, A_M (Eq. 16) is independent of cation concentrations:

$$A_M = \frac{k_0}{\nu_0}, \quad (20)$$

and Eq. 17 becomes

$$B_i = p_{Na} B_i^{Na} + p_{Ca} B_i^{Ca}, \quad (21)$$

Inserting explicitly the dependencies of the probabilities of cation occupancy given by Eq. 14, the latter equation becomes

$$B_i = \frac{([Na]/K_{Na}) B_i^{Na} + ([Ca]/K_{Ca}) B_i^{Ca}}{1 + ([Na]/K_{Na}) + ([Ca]/K_{Ca})}. \quad (22)$$

The solid line through the data in Fig. 6 *C* was drawn according to Eq. 22 for [Na] = 120 mM, K_{Na} = 34 mM, B_i^{Na} = 0.45; K_{Ca} = 0.16 mM, B_i^{Ca} = 0.78. The last three values were obtained from the least-squares fit of the data, whereas K_{Na} = 34 mM was imposed under the assumption that sodium ions inhibit TTX block by binding to the same site, where they (partially) antagonize the binding of labeled STX in rat brain preparations (Weigele and Barchi, 1978). Consistent with that choice, we find that our fitted value of K_{Ca} is close to the estimate of the high-affinity dissociation constant of Ca^{2+} for the same site (0.34 mM; Doyle et al., 1993).

For the sake of a later discussion, we notice that although we need to assume that extracellular Na^+ contributes to antagonizing TTX binding to fit our data, it is clear that TTX binding is dominated by the competition with Ca^{2+} down to [Ca] values comparable with K_{Ca}, so that the [Na] dependence of TTX block for [Ca] > 0.1 mM is expected to be very small. To illustrate this point, the dashed line in Fig. 6 *C* was calculated from Eq. 22, assuming that [Na] was reduced from 120 to 20 mM by substitution with a large noncompeting cation like $Tris^+$. It is seen that the two lines cross around [Ca] = 0.2 mM ($\sim K_{Ca} B_i^{Na}/(B_i^{Ca} - B_i^{Na})$), and that reducing [Na] for [Ca] > 0.2 mM does in fact slightly increase the amount of inhibited TTX binding affinity. This is because the reduced occupancy of the pore mouth by Na^+ increases the probability of occupancy by Ca^{2+}, which is an inhibitor that is twice as strong.

Antagonism of use dependence by intracellular cations

Conceptually, the trapped-ion model is qualitatively testable with experiments that antagonize use dependence by preventing the escape, or even stimulating the increase, of trapped cations. Notice that Schemes 1 and 3 predict use-dependent block in normal conditions on the basis of large cation occupancies of closed channels that are determined by the external concentrations, as opposed to the fact that open channels rapidly lose cations to the intracellular medium, where the latter have a lower electrochemical potential. Thus, Scheme 1 is physically sound for $\delta > 0$, only if the cyclic reaction U→L→H→U is associated with the inward transport of a cation along a negative electrochemical gradient. Therefore, reducing or reversing that gradient should antagonize or even reverse use dependence: opening TTX-blocked channels allows the binding of cations to the site in the outer pore lumen according to their intracellular electrochemical potential, and if this is higher than the extracellular potential, this may cause an increase in L states at the expense of H states.

This type of experiment is not as simple as it might appear. First of all, the escape of trapped calcium ions, which are the main cause of tonic inhibition at [Ca] ≥ 0.2 mM, is unavoidable (raising internal calcium activates chloride channels and makes the experiment impossible). According to Fig. 6 *C*, the partial inhibition at [Ca] = 0.2 mM is independent of [Na] and roughly equal to the maximum inhibition afforded by Na^+ trapping. Therefore, if we could stuff all blocked channels with trapped Na^+ from the internal medium, we expect that working at low [Ca], we would barely compensate the loss of Ca^{2+} inhibition. Second, we must consider that there are only two possibilities for a channel to trap a cation between a (outer) blocking TTX and a (inner) closed gate: either the channel is blocked by TTX while in a closed state and hosting a cation acquired from the extracellular medium (which is the case considered so far), or its outer mouth is already blocked by TTX and it closes while holding a cation acquired from the intracellular pool. Therefore, the capture of an internal Na^+ depends solely on the intracellular electrochemical potential of Na^+ existing when the channel closes, and it is strongly disfavored if closure occurs during the repolarization to very negative voltages that drive inward sodium currents.

The antagonism of TTX block by internal Na^+ can be demonstrated by comparing the effects induced by pulsing at voltages below or above the reversal potential for sodium currents, E_{rev}. Unlike the first, the second type of stimulus is expected to favor the occupancy of the pore by internal Na^+ and to attenuate thereby the use-dependent block caused by the loss of trapped Ca^{2+}. Two experiments of this type, which must be performed in patch-clamp to allow the recording of very fast activated outward currents, are shown in Fig. 7.

In the first experiment (Fig. 7, *A* and *B*), the extracellular solution in the recording pipette contained [Ca] = 1 mM, [Na] = 120 mM, and [T] = 30 nM TTX. Although the recordings were made without excising the patch, the *I-V* characteristic of the peak sodium currents (that reversed at $E_{rev} \approx 45$ mV and increased fairly linearly with voltage up to +100 mV) indicated that the cytoplasmic side of the patch was exposed to a medium with the same electrolytic composition as the bath (20 mM Na^+ and no divalent cations; the oocyte membrane was visibly broken in several places far from the region of the patch). A train of pulses with $V_P = 0$ mV and $T_P = 1$ ms elicited inward currents (left series of traces in Fig. 7 *A*) that decreased progressively and showed a cumulative extra block with $B_e = 0.42$ and $\tau = 15$ s (circles in Fig. 7 *B*). When the same protocol was applied by changing V_P to +100 mV, the outward currents elicited by the pulses (right series of traces in Fig. 7 *A*) showed a significantly smaller extra block with about the same time constant ($B_e = 0.31$, $\tau = 17$ s; diamonds in Fig. 7 *B*). This result shows indirectly the absence of significant artefacts due to cumulative inactivation, because these effects are expected to increase for pulses to +100 mV.

The value of B_e for the train at $V_P = 0$ mV is consistent with our previous analysis that predicts, for the above experimental conditions, a resting block inhibition of 0.58 that is totally removed independently of whether the activated channels close during the pulse or during the tail repolarization. However, for pulses to +100 mV a total loss of trapped cations is expected only for the fraction of blocked channels (~30%) that close during the tail. The remaining fraction, which closes during the pulse by inactivation, has a large probability of keeping a trapped Na^+ if it returns to the resting hyperpolarized state without reopening. In the experiment of Fig. 7, *A* and *B*, the lower extra block observed for $V_P = 100$ mV can be interpreted by assuming that pulses to +100 mV leave a residual block inhibition of 0.18 due to channels that close during a pulse having a probability of 0.6 of hosting a Na^+.

A more drastic case of antagonism of use dependence by outward electrochemical gradients is shown in the lower part of Fig. 7. In this experiment at [T] = 10 nM, the resting block inhibition was reduced by having [Ca] = 0.5 mM, and use dependence was stimulated by longer pulses ($T_P = 3$ ms) that caused full inactivation for $V_P = +100$ mV. Furthermore, the *I-V* characteristics showed $E_{rev} \approx 53$ mV and a strong reduction of the outward conductance (compare the ratios of the peak currents at 0 mV and at 100 mV

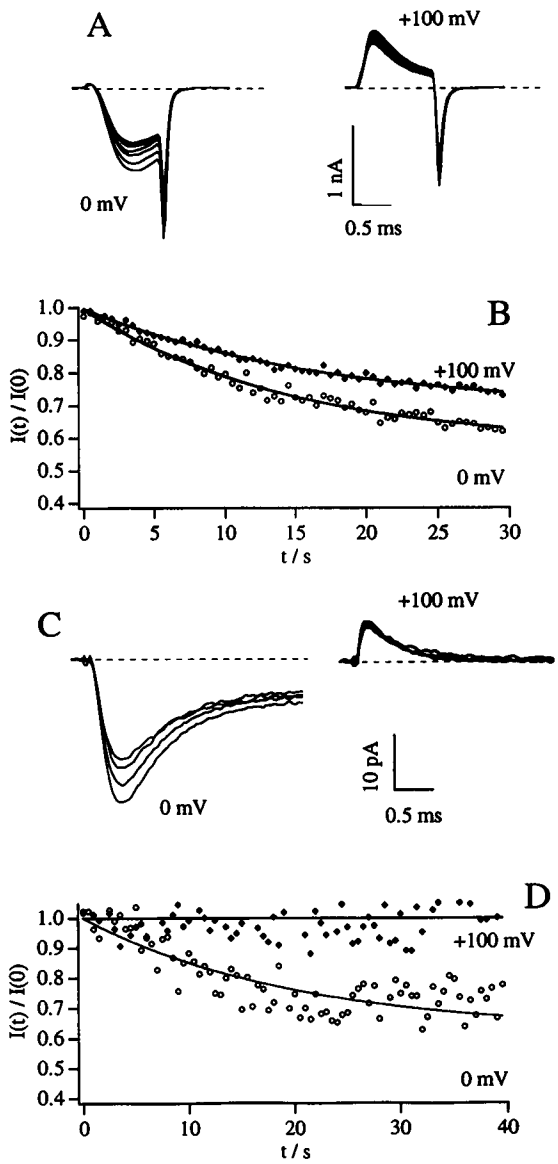

FIGURE 7 Antagonism of TTX use dependence by internal cations. (*A*) Superimposed records of sodium currents recorded from the same macropatch in a cell-attached configuration. The recording pipette was filled with NFR containing 1 mM Ca^{2+}, 30 nM TTX. The responses were elicited by a voltage pulse of 1 ms from $V_H = -120$ mV to $V_P = 0$ mV (*left*) or +100 mV (*right*). The traces show the first and every other 10th response to a train of 60 stimulations given at 0.5-s intervals, starting after a quiescent period of 3 min. (*B*) Plots of normalized decay of the peak amplitude recorded for the two different protocols in *A*. Smooth lines are least-squares fits of the data according to Eq. 1, with $B_e = 0.42$, $\tau = 15$ s ($V_P = 0$ mV) and $B_e = 0.31$, $\tau = 17$ s ($V_P = +100$ mV). (*C*) Superimposed patch clamp records from a different oocyte with protocols similar to *A*. The recording pipette contained NFR with 0.5 mM Ca^{2+} and 10 nM TTX. The stimulation pulses, from $V_H = -120$ mV, had $T_P = 3$ ms and $V_P = 0$ mV (*left*) or $V_P = +100$ mV (*right*). At $V_P = +100$ mV the outward sodium currents were completely inactivated during the pulse. The records shown are means of five responses taken at the beginning and every 13 s during a train of 80 stimulations given at 0.5-s intervals, starting after a quiescent period of 3 min. (*D*) Plot of the relative amplitude of the individual responses recorded during the train stimulation in *C*. The smooth line through the data at $V_P = 0$ mV is the least-squares fit according to Eq. 1 with $B_e = 0.37$, $\tau = 20$ s. The line through the data at $V_P = +100$ mV is a constant showing no use dependence.

in Fig. 7 *C* and in Fig. 7 *A*). This type of rectification (Pusch et al., 1989) is expected for an intact oocyte with an internal magnesium concentration close to that of the Barth's incubating medium (0.9 mM). The left-hand traces of Fig. 7 *C* show the usual use-dependent block stimulated by pulses to 0 mV, described in this case by $B_e = 0.37$ and $\tau = 20$ s (see Fig. 7 *D*, open circles). The right-hand traces of Fig. 7 *C* and the filled symbols in Fig. 7 *D* show the absence of extra block for stimulations to +100 mV, which drive outward currents and fully inactivate the channels during each pulse. Our interpretation is that at these voltages the loss of trapped Ca^{2+} by channels that open while being blocked is compensated by the uptake of Mg^{2+} that remains trapped when the channels close again by inactivation.

DISCUSSION

Our study of the use dependence of the TTX block in rat IIA sodium channels demonstrates that the trapped-ion mechanism, suggested by Salgado et al. (1986) for STX block in crayfish axons, allows a simple and viable quantitative model of the phenomenon. Our measurements in NFR solutions agree quantitatively with those reported by Patton and Goldin (1991) for the same preparation, but also show the same qualitative features of TTX and STX block in cardiac channels (Cohen et al., 1981; Carmeliet, 1987; Eickhorn et al., 1990; Makielski et al., 1993; Satin et al., 1994a) and frog node channels (Lönnendonker, 1989a,b, 1991a,b). Thus, we believe that the analysis developed in this work is generally applicable to the use-dependent block by guanidinium toxins of all voltage-gated sodium channels.

Estimates of the model parameters

According to our model, the parameters fitting extra block data yield estimates of the physical constants that characterize the interactions between TTX and cations and their respective receptors. Under the assumption of Eq. 19, which is fairly consistent with our data, Scheme 3 is defined quantitatively by six parameters: the second-order association rate constant of TTX, k_0; the three first-order dissociation rate constants, ν_0, ν_{Na}, and ν_{Ca}; and the two dissociation constants, K_{Ca} and K_{Na}. The values of these parameters that fit all of our data consistently are given in Table 2.

Our estimates of $\nu_0 \approx 19 \times 10^{-3}\ s^{-1}$, and $k_0 \approx 2\ \mu M^{-1}\ s^{-1}$, compare well with the "off" rate of $13 \times 10^{-3}\ s^{-1}$ and the "on" binding rate of 2.9 $\mu M^{-1}\ s^{-1}$, obtained from rapid-wash measurements in frog nodes at $V_H = -70$ mV (Ulbricht et al., 1986), where we expect most bound TTX to be in the H state. Our value for ν_0 was derived from Eq. 6 as the extrapolated rate of cumulative extra block at low [T], whereas k_0 was derived from Eq. 20 using the value of $A_M \approx 112\ \mu M^{-1}$, which best fits to Eqs. 6 and 7 the experimental [T] dependence of the rate and asymptotic level of extra block.

There are no estimates in the literature to compare with our guesses for the inhibition of TTX binding affinity due to the presence of Na^+ or Ca^{2+} in the outer pore lumen. We derive these guesses from the [Ca] dependence of extra block measurements, which are fitted by Eq. 22, assuming that Na^+ and Ca^{2+} reduce the affinity of TTX binding by ~45% and ~78%, respectively. According to Eq. 18, these specific inhibitions yield the estimates $\nu_{Na}/\nu_0 \approx 1.8$ and $\nu_{Ca}/\nu_0 \approx 4.4$. Thus, for consistency with the experimental observations, our model must assume that the repulsion by a trapped Na^+ and Ca^{2+} speeds the rate of TTX dissociation from its receptor by a factor of ~2 or ~4, respectively.

The closeness of our estimate of K_{Ca} to the value of 0.34 mM, obtained for the dissociation constant of Ca^{2+} or Mg^{2+} at the high affinity site of competition with radioactively labeled STX (Doyle et al., 1993), is an important test of the consistency of our model. On the other hand, in the data shown by Doyle et al. (1993), the largest displacement of STX by Na^+ (at 200 mM), or by Ca^{2+} or Mg^{2+} (at 20 mM), is less than 70% or 80%, respectively. Our analysis suggests that those data should be better fitted, assuming that a bound cation does not entirely prevent the binding of a toxin molecule.

We have no independent measurement of K_{Na}, because we have not explored [Na] dependencies for very low [Ca], where these measurements are meaningful. For this parameter we rely upon the estimate of ~34 mM, obtained from Na^+ competition with STX binding to rat brain synaptosomes (Weigele and Barchi, 1978).

Comparison with a state-dependent model of toxin binding

Our simplified Scheme 1 leads to analytical solutions that are formally identical to those obtainable from the three-state model used by Makielski et al. (1993) to describe phasic STX block of cardiac channels at very negative holding potentials. The latter model assumes a toxin-free resting state R, linked with rates k_{RC} and k_{CR} to a conditioned state C, from which the transition to the toxin-bound state B can occur with association and dissociation rate constants k_{CB} and k_{BC}; C represents a conformation of the channel in the activation pathway preceding the open state and long occupied during repolarization periods. It can be shown that this model predicts time dependencies, as in our Eqs. 1–3, and [T] dependencies, as in our Eqs. 5 and 6, provided we assign to our parameters the following expressions: $\nu_0 = k_{BC}$; $\nu = k_{CR} + k_{RC}$; $\delta = 0$; $A_M = k_{CB}/k_{BC}$; $B_i = k_{CR}/(k_{CR} + k_{RC})$. Using the estimates of Makielski et al. (1993) ($k_{BC} = 0.19\ s^{-1}$; $k_{CB} = 15.9\ s^{-1}\ \mu M^{-1}$; $k_{CR} = 1.75\ s^{-1}$; $k_{RC} = 0.88\ s^{-1}$), we expect that the phasic block by STX in cardiac channels can be accounted for by Scheme 1 with $\nu_0 = 0.19\ s^{-1}$; $\nu = 2.63\ s^{-1}$; $p_0k_0 = 4.5\ s^{-1}\ \mu M^{-1}$; $pk = 11.4\ s^{-1}\ \mu M^{-1}$.

Although consistent with the data of Makielski et al. (1993), our model does not postulate the existence of any

long-occupied intermediate state of activation, which is hardly compatible with the observation that the activation kinetics of repetitively stimulated channels are indistinguishable from those of long-rested ones (see, e.g., our patch-clamp recordings of Figs. 1 *B* and 7). Furthermore, the results of Fig. 7 are not easily reconcilable with use-dependence mechanisms involving peculiar conformations of the toxin receptor: inactivation per se cannot be thought to protect the receptor from reaching a high-affinity conformation, because this does not occur when inactivation develops at potentials that drive inward currents. An additional merit of our model is that of accounting, by the same mechanism and assuming a single toxin receptor site, both for the tonic block at very large hyperpolarization and for the extra block induced by prolonged depolarizations (Cohen et al., 1981). This is consistent with the finding that mutations, converting the cardiac toxin-resistant channel to the brain toxin-sensitive phenotype, strongly affect tonic and phasic block to a comparable degree (Satin et al., 1994a), and with the observation that recoveries from cumulative extra block or from the extra block induced by a long depolarization have practically identical time constants (Makielski et al., 1993).

Consistency of our model with previous observations

The trapped-ion idea that is the basis of our model has been overlooked by most authors because it appears to be qualitatively inconsistent with the observed dependence of extra block on membrane potential and on external cation concentrations. We discuss these observations below, arguing that they are not in quantitative disagreement with our model.

V_H dependence

Our data on the effect of V_H on TTX block are very close to those reported for the same preparation by Patton and Goldin (1991). Similar observations in cardiac channels have been reported as an increase in tonic block during long-lasting depolarizations (Carmeliet, 1987; Eickhorn et al., 1990) or as a slowly recovering extra block induced by long pulses (Cohen et al., 1981) and have been interpreted in various ways as indicating a higher toxin affinity for the activated and/or for the inactivated states of the sodium channel. In frog nodes, the amount of cumulative extra block is strongly V_H dependent and is readily measurable at $V_H < -70$ mV (Lönnendonker, 1989a), whereas both the rate of accumulation and the maximum toxin affinity under repetitive stimulation are V_H independent (Lönnendonker, 1989a,b). A strict correlation between cumulative extra block and inactivation, suggested by their similar range of steep V_H dependence, is excluded because strongly reducing inactivation with chloramine-T has little effect on extra block (Lönnendonker, 1991a).

Our V_H dependence and all analogous data in the literature are consistent with Schemes 1 or 3, which predict an increase in tonic block, and a consequent decrease in extra block, when the holding potential allows a steady rate of channel openings (δ) comparable to the rate of toxin dissociation from a cation-occupied channel (ν). Further depolarizations that cause a strong leak of trapped ions effectively eliminate cation-toxin interactions, thereby allowing a steady maximum toxin binding, so that no further block can be induced by depolarizing pulses. We estimate from our data that $\nu_{Ca} \approx 0.084\ s^{-1}$ and $\nu_{Na} \approx 0.034\ s^{-1}$ (see Table 2), and we have already argued that from single-channel data (Hirschberg et al., 1995) we expect the frequency of channel openings to be around these values right in the range of the observed steep V_H dependence of extra block. In our interpretation, the apparent correlation with inactivation may be just an indirect consequence of the fact that both processes are favored by channel opening (Armstrong and Bezanilla, 1977).

Dependence on pulse voltage

In contrast with its sharp decline at V_H values in the range where sodium channels tend to inactivate, the pulse-induced extra block depends on the pulse voltage like the activation of sodium conductance. Extra block induction and peak conductance activation curves are similarly affected by mutations of the channel protein (Patton and Goldin, 1991), but the activation of macroscopic conductance is systematically shifted toward more positive voltages. Because of this shift Patton and Goldin (1991) conclude that the inducement of extra block does not require the actual opening of the channels and must involve some conformational transition that precedes this event. Our analysis shows that this argument is incorrect, because the onset of extra block from the trapped-cation mechanism is linked to the probability of at least one channel opening, which may be large even for pulse voltages that yield small peak open-channel probabilities. The difference in the voltage dependence of the effect induced either by steady depolarizations or by short pulses, and the fact that induction of extra block has a lower threshold than the activation of macroscopic conductance, are both explained by our model by the same mechanism of removal of TTX-repelling ions from the only site where the toxin can bind: during steady depolarizations the removal of the inhibition increases according to the mean frequency at which a single channel opens, whereas a pulse depolarization reduces the cation repulsion according to the probability that a channel opens at least once during the pulse.

Dependence on external cations

Several authors find that the change in extra block associated with changes of the extracellular concentration of cations is smaller than qualitatively expected from the trapped-cation mechanism. Satin et al. (1994a) report that STX phasic block of rat heart channels expressed in oocytes "still

occurred in the absence of external Ca." It is not clear whether this observation was made with solutions containing Mg^{2+}, which is nearly as effective as calcium in causing extra block effects (Lönnendonker, 1991b; and our own data, not shown). Quite apart from this, the persistence of comparable extra block effects in the absence of calcium is consistent with our results and is attributed by our model to the remaining effect of TTX-Na^+ interaction. Conversely, Patton and Goldin (1991) argue against the trapped-cation model on the basis of their finding that replacing 80% of 96 mM Na^+ with $Tris^+$ in the presence of 1.8 mM Ca^{2+} and 1 mM Mg^{2+} slightly decreases the tonic block of TTX and does not significantly change the phasic block. In our model this result is consistent with the overwhelming role of divalent cations at these concentrations. Using the parameters that fit our [Ca]-dependence data, Eq. 8 predicts at [Na] = 96 mM a resting inhibition of the maximum toxin affinity by 70%, consistent with the finding of Patton and Goldin (1991) that the K_D for tonic block is about three times that for maximally stimulated block. At [Na] = 19 mM the prediction is that the resting inhibition increases to 73%, causing a 4% increase in phasic block and a 10% decrease in tonic block, in full agreement with the observations of Patton and Goldin (1991).

The effect of external Ca^{2+} and Mg^{2+} on STX use dependence has been studied in frog nodes by Lönnendonker (1991b). Although the experimental protocols and the analysis of the data are not easily comparable to ours, the reported effects are qualitatively similar to those that we observed for TTX block in our channels. The main difference, on the basis of which the author tends to discard the trapped-ion mechanism, is his finding that at $V_H \geq -110$ mV, extra block is virtually abolished by reducing [Ca] to 0.2 mM and it is not restored by doubling [Na]. We can tentatively reconcile this result with our model, noticing in the same paper that in frog nodes at [Ca] = 2 mM, STX extra block is reduced by half at ~ -105 mV and that, judging from the trend at increasing [Ca], this potential may be shifted negatively by more than 20 mV at [Ca] = 0.2 mM. Therefore, it is conceivable that extra block effects due to Na^+ trapping could not be observed in the range of hyperpolarizations explored by Lönnendonker (1991b).

Corollary considerations

Our analysis removes use dependence from the list of compelling objections to the view that the TTX binding site maintains a stable structure during the gating transitions of the sodium channel. Most interestingly, the basic phenomenon assumed by our model to underlie TTX use dependence, namely the repulsion between toxin molecules and cations bound in the outer pore, has previously been suggested to account for other apparent toxin-gating interactions. Indeed, the influence of TTX on the effects of local anesthetics (Cahalan and Almers, 1979) or thiazin dyes (Armstrong and Croop, 1982) is qualitatively consistent with TTX reducing the binding probability of external Ca^{2+} to a site from which it antagonizes the binding of positively charged molecules to the inner pore lumen on the other side of the selectivity filter. Likewise, the effects of STX and TTX on gating currents (Heggeness and Starkus, 1986; Keynes et al., 1991) could result indirectly from the competition between toxin molecules and outer-bound cations interacting electrostatically with charged gating structures (Heggeness and Starkus, 1986). Thus, none of the known effects of guanidinium toxins are inconsistent with the general idea that the toxins block the outer entrance of the pore binding to a vestibular structure that is not changed by gating transitions.

A direct effect on gating by calcium ions occupying the external pore lumen has been proposed by Armstrong and Cota (1991) on the basis of the close relationship between calcium-induced shifts of activation and calcium's tendency to block the channels. It is natural to identify the cation-binding site involved in TTX use dependence with that involved in the Ca^{2+} block of the open-channel conductance and in the cross-talk of Ca^{2+} with charged structures that gate the cytoplasmic entrance to the pore. Our finding that the dissociation constant estimated from use-dependence effects ($K_{Ca} \approx 0.16$ mM) is about two orders of magnitude lower than that estimated for calcium block of open channels ($K_{Ca}^{(O)} \approx 15$ mM at zero voltage; Pusch, 1990) is consistent with this view, because it implies a stronger binding of Ca^{2+} to the closed pore and an extra energy of $kT \ln(K_{Ca}^{(O)}/K_{Ca}) \approx 4\ kT$ to open a calcium-occupied channel. A rough estimate of the consequent shift in the activation curve can be obtained, assuming that bound Ca^{2+} hinders only a last, voltage-independent step in the activation pathway. Denoting as v_s the slope factor of the Boltzmann fit of the activation of conductance, we expect that the half-activation voltage for Ca^{2+}-occupied channels is shifted relative to that of Ca^{2+}-free channels by

$$\Delta V_{1/2} = v_s \ln(K_{Ca}^{(O)}/K_{Ca}).$$

For $K_{Ca} = 0.16$ mM, the latter relation is consistent with the data of Pusch (1990) on the effects of external calcium on wild-type rat brain IIA expressed in oocytes ($K_{Ca}^{(O)} \approx 15$ mM, $v_s \approx 10$ mV; and $\Delta V_{1/2} \approx 35$ mV for a change of [Ca] from 0.2 to 8 mM). Most interestingly, an S4 mutant with reduced voltage sensitivity (Stühmer et al., 1989) shows a 30% increase in both v_s and $\Delta V_{1/2}$, with no significant change in $K_{Ca}^{(O)}$ (Pusch, 1990), again in full agreement with the above relation. We conclude that the small dissociation constant of Ca^{2+} binding to closed channels needed to explain the calcium dependence of extra block is consistent with the idea that bound Ca^{2+} interacts with the cytoplasmic gates, as suggested by Armstrong and Cota (1991).

CONCLUDING REMARKS

The extracellular entrance to the ion pore is probably the best identified domain of the voltage-gated cation-selective chan-

nels. The use-dependent block of these channels by highly specific toxins provides an additional opportunity to study this domain by measuring the interaction between the toxins and bound cations, which we expect to be simply related to the effective electrical distance between the cation and the toxin in their bound positions. Our analysis suggests that the occupancy of the pore lumen by cations does not much affect the free-energy barrier for the "on" binding of TTX molecules, whereas the presence of trapped Na^+ or Ca^{2+} speeds the "off" rate by a factor of ~2 or ~4, lowering the activation energy for TTX dissociation by ~$0.7kT$ or ~$1.4kT$, respectively. The electrostatic repulsion between TTX and Na^+ or Ca^{2+} may account for these effects if the center of the TTX charge is placed at a distance of ~10 Å from the trapped cations and if the space in between has a dielectric constant of 80. These figures are not unreasonable, considering that the guanidinium group per se has a van der Waals radius of about 3 Å and that the dielectric constant of bulk water adequately describes the electrostatic interactions of charged residues in the outer mouth of K^+ channels with tightly bound charybdotoxin molecules (Stocker and Miller, 1994). Interestingly, if we interpret the data of Makielski et al. (1993) on STX use dependence according to our model, we estimate that Ca^{2+} speeds the rate of STX unbinding by a factor of about 14, slightly less than the factor of 19 (4.4^2) expected from doubling the toxin charge, but consistent with the second charge of STX being more remote from the Ca^{2+} binding site. It will be interesting to perform these studies on mutations of the pore domain of sodium channels (Terlau et al., 1991) and to investigate the possibility that similar use-dependent effects can be observed in appropriate conditions for the block of potassium channels by α-K-toxin peptides, the binding kinetics of which have been shown with a different method to be affected by external K^+ (Goldstein and Miller, 1993).

APPENDIX: STEADY-STATE AND TIME-DEPENDENT SOLUTIONS OF SCHEME 1

In reference to Scheme 1, let x, y, and $(1 - x - y)$ be the probabilities at any time of the states U, L, and H, respectively. The following differential equations govern the kinetics of the system:

$$\frac{dx}{dt} = -(\nu_0 + p_0k_0[T] + pk[T])x + (\nu - \nu_0)y + \nu_0 \tag{A1}$$

$$\frac{dy}{dt} = pk[T]x - (\nu + \delta)y. \tag{A2}$$

The steady-state solution, $\bar{x}$ and $\bar{y}$, obeys the conditions

$$0 = -(\nu_0 + p_0k_0[T] + pk[T])\bar{x} + (\nu - \nu_0)\bar{y} + \nu_0 \tag{A3}$$

$$0 = pk[T]\bar{x} - (\nu + \delta)\bar{y}, \tag{A4}$$

from which we obtain the following expression for $\bar{x}$:

$$\bar{x} = \frac{1}{1 + (p_0(k_0/\nu_0) + p(k/(\nu + \delta))((\nu_0 + \delta)/\nu_0))[T]}.$$

This equation is equivalent to Eq. 2 and yields the expression for the tonic block affinity, A_t, given in the text as Eq. 3.

Subtracting Eq. A1 from A3 and Eq. A2 from A4, we obtain

$$\frac{d(\bar{x} - x)}{dt} = -(\nu_0 + p_0k_0[T] + pk[T])(\bar{x} - x) + (\nu - \nu_0)(\bar{y} - y)$$

$$\frac{d(\bar{y} - y)}{dt} = pk[T](\bar{x} - x) - (\nu + \delta)(\bar{y} - y).$$

It is convenient to introduce the following change of variables:

$$x' = (\bar{x} - x)/\bar{x}; \quad y' = (\bar{y} - y)/\bar{y},$$

where x' can be also identified with the experimentally observable extra block probability, i.e., the fractional decrease in the number of toxin-free channels relative to the resting conditions. Using these definitions and Eq. A4, the above differential equations can be rewritten as

$$\frac{dx'}{dt} = -(\nu_0 + p_0k_0[T] + pk[T])x' + p\frac{k(\nu - \nu_0)}{\nu + \delta}[T]y'$$

$$\frac{dy'}{dt} = (\nu + \delta)(x' - y').$$

Considering the definitions of A_M and A_t, Eqs. 3 and 5, the first of the above equations can be rewritten as

$$\frac{dx'}{dt} = -\nu_0(1 + A_M[T])x' + \nu_0(A_M - A_t)[T]y'.$$

Using the expressions for τ and B_e given by Eqs. 6–8, the pair of differential equations that govern the relaxations of Scheme 1 can be finally conveniently rewritten as

$$\frac{dx'}{dt} = -\frac{1}{\tau}(x' - B_ey')$$

$$\frac{dy'}{dt} = (\nu + \delta)(x' - y') \tag{A5}$$

The general solution of Eq. A5 for constant external conditions has, for both x' and y', the form of a double exponential decay with rate constants λ_1 and λ_2 defined by the relations

$$\lambda_1 + \lambda_2 = \frac{1}{\tau} + \nu + \delta;$$

$$\lambda_1\lambda_2 = (1 - B_e)\frac{(\nu + \delta)}{\tau},$$

and satisfying the condition $\lambda_1 \le 1/\tau \le \lambda_2$. The first of the above relations provides an important test of the theory, predicting that the quantity $(\lambda_1 + \lambda_2 - 1/\tau)$ is independent of [T], in good agreement with the data in the last column of Table 1.

Any specific solution is determined by the initial values of x' and y'. Let them be $x'(0) = x'_0$ and $y'(0) = y'_0$. For the variable x' these values also set the initial condition: $(dx'/dt)_0 = -(x'_0 - B_ey'_0)/\tau$; and the solution can be conveniently expressed as

$$x'(t) = x'_0\omega(t) + y'_0B_e\varphi(t), \tag{A6}$$

where $\omega(t)$ and $\varphi(t)$ are double-exponential functions defined by

$$\omega(t) = \frac{(\lambda_2 - (1/\tau))e^{-\lambda_1 t} + ((1/\tau) - \lambda_1)e^{-\lambda_2 t}}{\lambda_2 - \lambda_1}$$

$$\varphi(t) = \frac{(e^{-\lambda_1 t} - e^{-\lambda_2 t})}{\tau(\lambda_2 - \lambda_1)}. \quad \text{(A7)}$$

Notice that $\omega(t)$ and $\varphi(t)$ are both positive for $t > 0$. $\omega(t)$ decreases monotonically from $\omega(0) = 1$ with initial derivative $(d\omega/dt)_0 = -1/\tau$; $\varphi(t)$ increases from $\varphi(0) = 0$ with initial derivative $(d\varphi/dt)_0 = 1/\tau$ and reaches a peak at $t = t_p$, characterized by $(\lambda_2 - \lambda_1)t_p = \ln(\lambda_2/\lambda_1)$; $\varphi(t_p) = e^{-\lambda_1 t_p}/\lambda_2\tau < 1$.

Extra block induced by a single stimulus

Let us indicate with π the probability that a channel opens at least once during the stimulus. For a channel blocked in state L, π is also the probability of losing the trapped ion and switching to the H state. Therefore, the probability of state L immediately after the stimulus is $y_0 = \bar{y}(1 - \pi)$ and the initial condition for y' is $y'_0 = (\bar{y} - y_0)/\bar{y} = \pi$. On the other hand, because binding and unbinding reactions occur on a time scale of seconds, the number of toxin-free channels does not change significantly during the pulse, so that the initial condition for x' is $x_0' = 0$. In this case Eq. A6 yields

$$x'(t) = \pi B_e \varphi(t).$$

Considering the definition of $\varphi(t)$ and that, according to Eqs. 6 and 7, $B_e/\tau = \nu_0 B_t A_M[T]$, the comparison of the above equation with Eq. 11 yields the expression for the experimental parameter C given in the text (Eq. 12).

Cumulative extra block

The typical protocol revealing the use-dependent block consists of successive stimulations applied at constant time intervals, ϑ, starting from resting conditions. Let us number successive pulses starting from 0, and denote with x'_n and y'_n the values of x' and y' at the onset of pulse n. As argued previously, the value of x' after the pulse is still x'_n, whereas the stimulus changes the L-state probability by a factor $(1 - \pi)$, causing y' to jump to the new value: $\pi + (1 - \pi)y'_n$. Normally experimental protocols apply strong pulses, for which $\pi = 1$. In this case, at the beginning of any interpulse period we always have $y' = 1$, and Eq. A6 yields a simple recurrent relation between x'_n and x'_{n+1}:

$$x'_{n+1} = \omega(\vartheta)x'_n + B_e\varphi(\vartheta).$$

Using the initial condition $x'_0 = 0$ (resting conditions before pulse 0), and omitting ϑ for simplicity, this relation yields

$$x'_n = (1 + \omega + \omega^2 + \ldots + \omega^{(n-1)})B_e\varphi$$

or

$$x'_n = \frac{B_e\varphi}{1 - \omega}(1 - \omega^n).$$

Introducing the real time, $t = n\vartheta$, this equation becomes

$$x'(t) = B_\vartheta(1 - e^{-t/\tau_\vartheta}),$$

where the asymptotic extra block probability, B_ϑ, and its time constant, τ_ϑ, have the following dependence on the stimulation interval ϑ:

$$B_\vartheta = B_e\frac{\varphi(\vartheta)}{1 - \omega(\vartheta)} \quad \text{(A8)}$$

$$\tau_\vartheta = -\frac{\vartheta}{\ln[\omega(\vartheta)]}. \quad \text{(A9)}$$

Equations A7–A9 have been used to fit the data of Fig. 2. Considering the properties of the functions ω and φ, it is easily verified that B_e and τ are indeed the limiting values of B_ϑ and τ_ϑ for $\vartheta \to 0$.

Recovery from cumulative extra block

The recovery of the resting population of unblocked channels after the end of a saturating train stimulation is obtained from Eq. A6 using the initial conditions $x'_0 = B_e$, $y'_0 = 1$. This yields

$$x'(t) = B_e[\omega(t) + \varphi(t)],$$

or, according to Eq. A7,

$$x'(t) = B_e\frac{\lambda_2 e^{-\lambda_1 t} - \lambda_1 e^{-\lambda_2 t}}{\lambda_2 - \lambda_1}.$$

Considering the meaning of the variable x', the last equation is identical to Eq. 13, used for the fit of recovery from saturated extra block.

We thank K. Imoto for providing cRNA and E. Gaggero for technical assistance in setting up the voltage clamp.

Supported by the Progetto Finalizzato Ingegneria Genetica, CNR. MP was the recipient of research grant SC1*305 from the EEC.

REFERENCES

Armstrong, C. M., and F. Bezanilla. 1977. Inactivation of the Na channel. II. Gating current experiments. *J. Gen. Physiol.* 70:567–590.

Armstrong, C. M., and C. Cota. 1991. Calcium ion as a cofactor in Na channel gating. *Proc. Natl. Acad. Sci. USA.* 88:6528–6531.

Armstrong, C. M., and R. S. Croop. 1982. Simulation of Na channel inactivation by thiazin dyes. *J. Gen. Physiol.* 80:641–662.

Baer, M., P. M. Best, and H. Reuter. 1976. Voltage-dependent action of tetrodotoxin in mammalian cardiac cells. *Nature.* 263:344–345.

Butterworth IV, G. F., and G. R. Strichartz. 1990. Molecular mechanisms of local anesthesia: a review. *Anesthesiology.* 72:711–734.

Cahalan, M. D., and W. Almers. 1979. Interactions between quaternary lidocaine, the sodium channel gates, and tetrodotoxin. *Biophys. J.* 27: 39–56.

Carmeliet, E. 1987. Voltage-dependent block by tetrodotoxin of the sodium channel in rabbit cardiac Purkinje fibbers. *Biophys. J.* 51:109–114.

Cohen, C. J., B. P. Bean, T. J. Colatsky, and R. W. Tsien. 1981. Tetrodotoxin block of sodium channels in rabbit Purkinje fibers. Interactions between toxin binding and channel gating. *J. Gen. Physiol.* 78:383–411.

Courtney, K. R. 1975. Mechanisms of frequency-dependent inhibition of sodium currents in frog myelinated nerve by the lidocaine derivatives GEA 968. *J. Pharmacol. Exp. Ther.* 195:225–236.

Doyle, D. D., Y. Guo, S. L. Lustig, J. Satin, R. B. Rogart, and H. A. Fozzard. 1993. Divalent cation competition with [^{3}H]saxitoxin binding to tetrodotoxin-resistant and -sensitive sodium channels: a two-site structural model of ion/toxin interaction. *J. Gen. Physiol.* 101:153–182.

Eickhorn, R., J. Weirich, D. Hornung, and H. Antoni. 1990. Use dependence of sodium current inhibition by tetrodotoxin in rat cardiac muscle: influence of channel state. *Pflugers Arch.* 416:398–405.

Goldstein, S. A. N., and C. Miller. 1993. Mechanism of charybdotoxin block of a voltage-gated K^+ channel. *Biophys. J.* 65:1613–1619.

Heggeness, S. T., and J. G. Starkus. 1986. Saxitoxin and tetrodotoxin. Electrostatic effects on sodium channel gating current in crayfish axons. *Biophys. J.* 49:629–643.

Heinemann, S. H., H. Terlau, W. Stühmer, K. Imoto, and S. Numa. 1992. Calcium channel characteristics conferred on the sodium channel by single mutations. *Nature.* 356:441–443.

Hidalgo, P., and R. MacKinnon. 1995. Revealing the architecture of a K^+ channel pore through mutant cycles with a peptide inhibitor. *Science.* 268:305–310

Hille, B. 1975. The receptor for tetrodotoxin and saxitoxin: a structural hypothesis. *Biophys. J.* 15:615–619.

Hille, B. 1992. Ionic Channels of Excitable Membranes. Sinauer Associates, Sunderland, MA.

Hirschberg, B., A. Rovner, M. Liebermann, and J. Patlak. 1995. Transfer of 12 charges is needed to open skeletal muscle Na^+ channels. *J. Gen. Physiol.* 106:1053–1068.

Horn, R., C. A. Vandenberg, and K. Lange. 1984. Statistical analysis of single sodium channels. Effects of *N*-bromoacetamide. *Biophys. J.* 45: 323–335.

Kao, C. Y. 1986. Structure activity relations of tetrodotoxin, saxitoxin, and analogues. *Ann. N.Y. Acad. Sci.* 479:52–67.

Keynes, R. D., N. G. Greeff, I. C. Forster, J. M. Bekkers. 1991. The effect of tetrodotoxin on the sodium gating current in the squid giant axon. *Proc. R. Soc. Lond. B.* 246:135–140.

Kontis, K. J., and A. L. Goldin. 1993. Site-directed mutagenesis of the putative pore region of the rat IIA sodium-channel. *Mol. Pharmacol.* 43:635–644.

Lipkind, G. M., and H. A. Fozzard. 1994. A structural model of the tetrodotoxin and saxitoxin binding site of the sodium channel. *Biophys. J.* 66:1–13.

Lönnendonker, U. 1989a. Use-dependent block of sodium channels in frog myelinated nerve by tetrodotoxin and saxitoxin at negative holding potentials. *Biochim. Biophys. Acta.* 985:153–160.

Lönnendonker, U. 1989b. Binding of tetrodotoxin and saxitoxin to Na^+ channels at different holding potentials: fluctuation measurements in frog myelinated nerve. *Biochim. Biophys. Acta.* 985:161–167.

Lönnendonker, U. 1991a. Use-dependent block with tetrodotoxin and saxitoxin at frog Ranvier nodes. I. Intrinsic channel and toxin parameters. *Eur. Biophys. J.* 20:135–141.

Lönnendonker, U. 1991b. Use-dependent block with tetrodotoxin and saxitoxin at frog Ranvier nodes. II. Extrinsic influence of cations. *Eur. Biophys. J.* 20:143–149.

Lönnendonker, U., B. Neumcke, and R. Stämpfli. 1990. Interaction of monovalent cations with tetrodotoxin and saxitoxin binding at sodium channels of frog myelinated nerve. *Pflugers Arch.* 416:750–757.

Makielski, J. C., J. Satin, and Z. Fan. 1993. Post-repolarization block of cardiac sodium channels by saxitoxin. *Biophys. J.* 65:790–798.

Methfessel, C., V. Witzemann, T. Takahashi, M. Mishina, S. Numa, and B. Sakmann. 1986. Patch clamp measurements on *Xenopus* laevis oocytes: currents through endogenous channels and implanted acetylcholine receptor and sodium channels. *Pflugers Arch.* 407:577–588

Narahashi, T. 1974. Chemicals as tools in the study of excitable membranes. *Physiol. Rev.* 54:813–889.

Noda, M., T. Ikeda, T. Kayano, H. Suzuki, H. Takeshima, M. Kurasaki, H. Takahashi, and S. Numa. 1986. Existence of distinct sodium channel messenger RNAs in rat brain. *Nature.* 320:188–192.

Noda, M., H. Suzuki, S. Numa, and W. Stühmer. 1989. A single point mutation confers tetrodotoxin and saxitoxin insensitivity on the sodium channel II. *FEBS Lett.* 259:213–216.

Patton, D. E., and A. L. Goldin. 1991. A voltage-dependent gating transition induces use-dependent block by tetrodotoxin of rat IIA sodium channels expressed in *Xenopus* oocytes. *Neuron.* 7:637–647.

Pusch, M. 1990. Divalent cations as probes for structure-function relationships of cloned voltage-dependent sodium channels. *Eur. Biophys. J.* 18:327–333.

Pusch, M., F. Conti, and W. Stühmer. 1989. Intracellular magnesium blocks sodium outward currents in a voltage- and dose-dependent manner. *Biophys. J.* 55:1267–1271.

Pusch, M., M. Noda, W. Stühmer, S. Numa, and F. Conti. 1991. Single point mutations of the sodium channel drastically reduce the pore permeability without preventing its gating. *Eur. Biophys. J.* 20:127–133.

Salgado, V. L., J. Z. Yeh, and T. Narahashi. 1986. Use- and voltage-dependent block of the sodium channel by saxitoxin. *Ann. N.Y. Acad. Sci.* 479:84–95.

Satin, J., J. W. Kyle, M. Chen, P. Bell, L. L. Cribbs, H. A. Fozzard, and R. B. Rogart. 1992. A mutant of TTX-resistant cardiac sodium channels with TTX-sensitive properties. *Science.* 256:1202–1205.

Satin, J., J. W. Kyle, Z. Fan, R. Rogart, H. A. Fozzard, and J. C. Makielski. 1994a. Post-repolarisation block of cloned sodium channels by saxitoxin: the contribution of pore-region amino acids. *Biophys. J.* 66:1353–1363.

Satin, J., J. T. Limbers, J. W. Kyle, R. Rogart, and H. A. Fozzard. 1994b. The saxitoxin tetrodotoxin binding-site on cloned rat-brain IIA Na^+ channels is in the transmembrane electric-field. *Biophys. J.* 67: 1007–1014.

Stocker, M., and C. Miller. 1994. Electrostatic distance geometry in a K^+ channel vestibule. *Proc. Natl. Acad. Sci. USA.* 91:9509–9513.

Strichartz, G. R. 1973. The inhibition of sodium currents in myelinated nerve by quaternary derivatives of lidocaine. *J. Gen. Physiol.* 62:37–57.

Stühmer, W., F. Conti, H. Suzuki, X. Wang, M. Noda, N. Yahagi, H. Kubo, and S. Numa. 1989. Structural parts involved in activation and inactivation of the sodium channel. *Nature.* 339:597–603.

Stühmer, W., C. Methfessel, B. Sakmann, M. Noda, and S. Numa. 1987. Patch clamp characterization of sodium channels expressed from rat brain cDNA. *Eur. Biophys. J.* 14:131–138.

Terlau, H., S. H. Heinemann, W. Stühmer, M. Pusch, F. Conti, K. Imoto, and S. Numa. 1991. Mapping the site of block by tetrodotoxin and saxitoxin toxins of sodium channel II. *FEBS Lett.* 293:93–96.

Ulbricht, W., H. H. Wagner, and J. Schmidtmayer. 1986. Kinetics of TTX-STX block of sodium channels. *Ann. N.Y. Acad. Sci.* 479:68–83.

Weigele, J. B., and R. L. Barchi. 1978. Saxitoxin binding to the mammalian sodium channel. Competition by monovalent and divalent cations. *FEBS Lett.* 95:49–53.